Chemical Engineering Science 318 (2025) 122219

Contents lists available at ScienceDirect

Chemical Engineering Science

journal homepage: www.elsevier.com/locate/ces

Considerations for the optimization of biocatalyst formulation in multi-enzymatic reactions: Co-immobilized enzymes advantages depend on enzyme kinetic properties

Diego Carballares [a], John M. Woodley [b,*], Roberto Fernandez-Lafuente [c,*], Juan M. Bolivar [a,*]

[a] FQPIMA Group, Chemical and Materials Engineering Department, Faculty of Chemical Sciences, Complutense University of Madrid, Madrid 28040, Spain
[b] Department of Chemical and Biochemical Engineering, Technical University of Denmark, 2800 Kgs Lyngby, Denmark
[c] Departamento de Biocatálisis, ICP-CSIC, C/ Marie Curie 2, Campus UAM-CSIC Cantoblanco, Madrid 28049, Spain

ARTICLE INFO

Keywords:
Cascade biocatalysis
Co-immobilized enzymes
Biocatalyst optimization metrics
Kinetic modeling and constants
Mass transfer limitations
Initial rate vs. final yield

ABSTRACT

The design of combi-biocatalyst for optimizing cascade reactions is challenging, particularly in terms of the choice of the biocatalyst formulations, including the relative amounts of enzymes to be used, and the experimental set-up strategy chosen for optimization. This paper demonstrates, via dynamic simulation, the optimization of a combi-biocatalyst designed for a multi-cascade two-reaction series (A → B, B → C) involving two enzymes (E1, E2) in free, individually immobilized, or co-immobilized formulations. This has been analyzed in three different scenarios: (1) K_M is identical for both enzymes (i.e. $K_{M1} = K_{M2}$), (2) $K_{M1} > K_{M2}$, and (3) $K_{M1} < K_{M2}$. The ratio of mass transport and reaction times was defined using a modified Thiele modulus, providing a useful metric to evaluate the relative magnitude of mass transport limitations. Global mass transport was considered. In the absence of mass transport limitations, the three catalyst formulations gave identical results. However, when (moderate) mass transport limitations were included, substrate (A) and intermediate (B) concentration gradients appear, meaning that the multi-enzyme catalyst formulation becomes critical. The results indicate that although enzyme co-immobilization always provides some kinetic advantages compared to the use of individually immobilized enzymes, these advantages increased when $K_{M2} < K_{M1}$ and vice versa. The first situation also provides the most efficient combi-biocatalyst. The optimal enzyme ratio in all enzyme formulations, determined by using either initial rates or time to reach the target yield, is in some instances quite different. This suggests that, although more time-consuming, the latter parameter should be utilized in the design of the enzyme mass ratio for the combined biocatalysts. The optimal enzyme ratio depends on the enzyme formulation. Therefore, extrapolating the results achieved using individually immobilized enzymes to co-immobilized biocatalysts can lead to the preparation of a biocatalyst with sub-optimal efficiency.

1. Introduction

Today, enzyme-mediated catalysis is becoming increasingly relevant in both academia and also industry, due to excellent reactions rates under mild conditions, combined with high selectivity and specificity (Choi et al., 2015; Sheldon and Pereira, 2017; Sheldon and Woodley, 2018; Wu et al., 2021). One of the areas currently receiving particular attention is the design of cascade reactions, processes where the product of one enzyme acts as the substrate for the subsequent one in a chain reaction, mimicking the metabolic pathways occurring naturally in cells (France et al., 2017; Lopez-Gallego and Schmidt-Dannert, 2010; Pizarro et al., 2012; Schrittwieser et al., 2018). Such cascade reactions, involving several enzymes, enable very complex modifications, transforming simple substrates into quite complex (and valuable) products.

The success of a biocatalytic process largely depends on the design of an effective biocatalyst. During biocatalyst design, the enzyme can be selected from any number of active proteins from an enormous range of biodiversity (Fernández-Arrojo et al., 2010), and the target features may be improved by protein engineering using either directed evolution (Arnold, 2018; Bornscheuer and Pohl, 2001; Renata et al., 2015), site-

* Corresponding authors.
E-mail addresses: jw@kt.dtu.dk (J.M. Woodley), rfl@icp.csic.es (R. Fernandez-Lafuente), juanmbol@ucm.es (J.M. Bolivar).

https://doi.org/10.1016/j.ces.2025.122219
Received 14 April 2025; Received in revised form 10 July 2025; Accepted 12 July 2025
Available online 13 July 2025

directed mutagenesis (Drufva et al., 2021), or combinations thereof. With the current interest in cascade reactions, the preparation of enzymes bearing several active centers by genetic tools also has great relevance (Carballares et al., 2022a) (e.g., plurizymes (Alonso et al., 2020; Fernandez-Lopez et al., 2022)). Complementary to molecular biology strategies, enzyme immobilization is a further option to improve many enzyme properties (Bolivar et al., 2022), and is also complementary to protein engineering (Bernal et al., 2018; Rodrigues et al., 2014). Immobilization was initially developed to facilitate enzyme recovery and reuse, enabling the advantages of heterogeneous (metal) catalysts to be used also with enzymes (e.g., enlarging the possibilities of reactors to be used for the process and increasing the control of the reaction) (Bolivar et al., 2022; Sheldon and van Pelt, 2013). Subsequently, it was suggested that immobilization could be far more useful for biocatalyst design than solely for these points, enabling many other enzyme features to be improved (Bolivar et al., 2022; Sheldon and van Pelt, 2013). Nevertheless, it is important to recognize that aside from improving enzyme properties, the ability to recover enzyme effectively at the end of a reaction (whether to improve downstream processing, fulfil regulatory requirements, or for recycle) remains a major challenge, and one where immobilization has a particular role to play (Bolivar et al., 2022; Di Cosimo et al., 2013; Liese and Hilterhaus, 2013; Sheldon and van Pelt, 2013). The most usual enzyme property that scientists aim to improve via immobilization is stability (Bilal et al., 2019a; Rodrigues et al., 2021; Wahab et al., 2020). Firstly, to include and disperse enzyme molecules inside a porous support is enough to prevent it from interacting with external surfaces and interfaces, or from suffering intermolecular processes, and this can directly improve the enzyme operational stability (Bilal et al., 2019a; Rodrigues et al., 2021; Wahab et al., 2020). Secondly, multi-point immobilization can also increase enzyme rigidity, multi-subunit immobilization can avoid subunit dissociation in multimeric enzymes, and immobilization can reduce other causes of inactivation (Bilal et al., 2019a; Rodrigues et al., 2021; Wahab et al., 2020). Properly designed enzyme immobilization also permits enzyme purification, saving costs in the biocatalyst production (Barbosa et al., 2015). Moreover, as the immobilization very likely will produce some enzyme distortions, the enzyme selectivity, specificity, activity, inhibition, etc. can all be altered (Bilal et al., 2019b; Rodrigues et al., 2013). In this way, this step in the preparation of a biocatalyst attracts growing interest in the scientific community, and is a fundamental step in the design of many industrial biocatalytic processes (Bolivar et al., 2022).

In the context of enzyme cascades, enzyme co-immobilization has also received great attention (Hwang and Lee, 2019; Ren et al., 2019; Schmid-Dannert and López-Gallego, 2019; Velasco-Lozano and López-Gallego, 2018; Xu et al., 2020). This consists of the immobilization of two (or more) enzymes in the same porous particle, as this is expected to improve the initial reaction rate of product formation (since the biocatalyst particle will bear all involved active centers) (Hwang and Lee, 2019; Ren et al., 2019; Schmid-Dannert and López-Gallego, 2019; Velasco-Lozano and López-Gallego, 2018; Xu et al., 2020). These kinetic improvements were initially linked to the "proximity" of the co-immobilized enzymes, but there are some reports that refute this argument (Idan and Hess, 2013a, 2013b, 2012; Xiong et al., 2022; Zhang et al., 2016). These reports show that the main effect of using co-immobilized enzymes in porous supports is the increase of the intermediate concentrations in the confined space where the enzymes are co-immobilized, as these intermediates, substrates of the other enzymes in the cascade, are *in-situ* produced in this confined space (Idan and Hess, 2013a, 2013b, 2012; Monteiro et al., 2022; Xiong et al., 2022; Zhang et al., 2016). In this way, due to product diffusional limitations, enzyme co-immobilization can increase the substrate concentration in the surroundings of the all the co-immobilized enzymes involved in the cascade. Hence, all the co-immobilized enzymes that are located after the first enzyme in the reaction chain will be exposed to high concentrations of their respective substrates from the beginning of the reaction, perhaps even saturating concentrations. Using individually immobilized enzymes, the second and successive enzymes in the reaction cascade will not have available substrate in the first moments of the reaction, and a lag time is usually observed, where there is no formation of the target product (Arana-Peña et al., 2021).

However, the kinetic gains achieved by enzyme co-immobilization, mainly related to the initial reaction rate, must also compensate some problems in the design and handling of the co-immobilized biocatalyst (Arana-Peña et al., 2021). It may not be easy to take full advantage of the enzyme immobilization for all involved enzymes if we use the same support surface for all the enzymes (Arana-Peña et al., 2021). And, as stated above, a proper immobilization may be a key point in the preparation of a suitable biocatalyst. Moreover, it is likely that the stability of all involved co-immobilized enzymes does not fit, and that when the least stable enzyme has reached a level of deactivation that makes it necessary to discard, other co-immobilized enzymes may remain fully active (Arana-Peña et al., 2021). That is, the discarding of fully active immobilized enzymes may be necessary. There are some strategies to avoid this problem (Arana-Peña et al., 2021,2022; Carballares et al., 2022b; Morellon-Sterling et al., 2021), but even in the best case, this necessitates the use of more sophisticated (and more expensive) enzyme immobilization strategies. Moreover, the maintenance of the reaction cycle time when some enzymes are inactivated is more complex when using co-immobilized enzymes rather than individually immobilized ones, and recent theoretical and experimental approaches have provided advances in understanding and design of multi-enzymatic systems in free and immobilized form (Høst et al., 2022; Paschalidis et al., 2023; (Paschalidis et al., 2024)). Hence, the decision on the use of co-immobilized or individually immobilized enzymes must be taken considering many different factors.

In some cases, e.g., if some intermediates must be instantaneously modified by the next enzyme in the chain due to their instability (Butò et al., 1994; Chmura et al., 2013; Fernández-Lafuente et al., 1998; Mateo et al., 2006; Upadhya et al., 1999; Van Rantwijk et al., 2008), enzyme co-immobilization is unavoidable, even with the problems that co-immobilization can present. However, when just a kinetic gain is intended, affecting mainly the initial reaction rate and the initial reaction course, it could be interesting to know what the magnitude of these kinetic improvements is in each specific case. The gains produced by enzyme co-immobilization must depend on the Michaelis-Menten constant (K_M) of the involved enzymes, the enzyme mass activities in the biocatalyst and the accumulation of the intermediate in the combi-biocatalyst particle by diffusion (dependent on the diffusion coefficients of the involved reactants inside the porous biocatalyst particle and the particle size).

A critical aspect in the rational design of the ratio of the amounts of both enzymes in the combi-biocatalyst is the choice of the optimization criterion. In the applied biocatalysis community, the most commonly used approach is to determine the initial reaction rates for each biocatalyst formulation (Hwang and Lee, 2019; Ren et al., 2019; Schmid-Dannert and López-Gallego, 2019; Velasco-Lozano and López-Gallego, 2018; Xu et al., 2020). This approach is widely adopted because it requires shorter experiments and considers that this is directly related to the reaction course. However, we consider that optimizing based solely on initial reaction rates can be misleading, as this metric does not capture the full dynamics of substrate depletion and intermediate accumulation throughout the reaction. The cycle time—the time required to achieve a desired yield or complete conversion is the really important parameter, but these values are harder to determine and require more time, effort and resources. Our hypothesis is that these two approaches can lead to different optimal enzyme ratios, especially in systems where kinetic asymmetry or diffusional limitations play a significant role. Therefore, while initial rate screening is valuable for rapid evaluation, assessing cycle time or overall productivity may be necessary for robust combi-biocatalyst design, particularly in processes where yield and throughput are critical.

Based on the previous assumptions, we present here a theoretical

analysis of cascade biocatalyst systems with varying K_M values for the two enzymes, covering cases where K_M values are identical, or where $K_{M2} > K_{M1}$ or vice versa. Our analysis specifically focuses on kinetic regimes where the initial substrate concentration is of the same order of magnitude as the K_M values of the enzymes. This allows us to deliberately examine the system under intermediate (mixed-order) kinetic conditions, where neither zero-order nor first-order kinetics dominate, and both substrate and enzyme critically influence reaction behavior. We systematically compare the performance of free, individually immobilized, and co-immobilized enzyme formulations, and highlight the optimal enzyme ratios predicted under different kinetic and transport regimes, using both initial rate and cycle time as criteria. To focus on the effects of K_M asymmetry and mass transport, we assume identical k_{cat} for both enzymes and neglect enzyme inhibition or deactivation. These simplifications allow us to isolate the impact of kinetic and diffusional parameters, while acknowledging that k_{cat} variation and enzyme stability can also affect optimal design in practical systems. By clarifying these relationships, our study provides new insight into when co-immobilization is truly advantageous and guides the rational selection of enzyme pairs and process strategies for multi-enzymatic cascades. All simulations are based on a two-enzyme cascade model system (Fig. 1), with the further assumption that immobilization does not alter enzyme properties, and only diffusional limitations are considered.

2. Methods

2.1. Mathematical model and assumptions

A mathematical model was developed to analyze the performance of a biocatalyst in a multi-enzymatic cascade reaction involving two enzymes under three different formulations: free enzymes, enzymes individually immobilized in different particles, and enzymes co-immobilized in the same particle. The model was implemented in Berkeley Madonna 10 using the fourth-order Runge-Kutta (RK4) numerical integration method with a time step (Δt) of 0.001 time units for all enzyme formulations.

The reaction system proposed was

$A \rightarrow B$ Reaction (1) catalyzed by E_1.

$B \rightarrow C$ Reaction (2) catalyzed by E_2.

The model assumes that both enzymes follow Michaelis-Menten kinetics, with a maximum specific activity (k_{cat}) for both enzymes and three different scenarios regarding the Michaelis-Menten constant (K_M): (i) identical K_M values for both enzymes (i.e. $K_{M1} = K_{M2}$), (ii) $K_{M1} > K_{M2}$ and (iii) $K_{M2} > K_{M1}$. To isolate the effects of K_M asymmetry and mass transport resistance, the catalytic turnover numbers (k_{cat}) for both enzymes were fixed at the values indicated beneath. No enzyme inhibition or deactivation was considered. These simplifications allow direct comparison across scenarios, but we acknowledge that in real systems, k_{cat} values and enzyme stability can vary substantially and influence biocatalyst performance.

It was modelled as follows.

2.1.1. Free enzymes

The reaction kinetics were defined as:

$$r_1 = \frac{V_{max1} \cdot A}{K_{M1} + A} \tag{1}$$

$$r_2 = \frac{V_{max2} \cdot B}{K_{M2} + B} \tag{2}$$

Where the maximum velocities are

$$V_{max1} = e_1 k_{cat1} \tag{3}$$

$$V_{max2} = e_2 k_{cat2} \tag{4}$$

r_1, r_2, V_{max1}, V_{max2} display units of specific reaction rate (per unit of mass of catalyst). A and B are the concentrations of the components A and B (in units of moles per unit of volume). e_1 and e_2 represent the ratio between the concentrations of the enzyme 1 or 2 and the total enzyme concentration, E_T (defined as 1 unit of mass of enzyme per unit of volume). $kcat_1$ and $kcat_2$ are maximum specific activities. To facilitate data in-silico visualization, the following data has been used as basis for calculation: $kcat_1 = kcat_2 = 10$ μmol min^{-1} mg^{-1}, and $E_T = 1$ mg ml^{-1} and initial concentration of $A = 100$ mM. The batch reaction was simulated with $A_0 = 100$ mM, $B_0 = 0$, $C_0 = 0$. In all cases, this initial substrate concentration was selected to be of the same order of magnitude as the K_M values of the first reaction ($A_0/K_M = 2$). This approach allows us to capture the effects of both substrate and enzyme properties on cascade performance and avoids the limiting cases where only zero-order or first-order behavior would dominate. Three representative K_M values (5, 50, 500 mM) were examined for the second reaction to cover extreme affinity ranges.

The substrate and product balances were defined as assuming a well-mixed system without mass transfer limitations:

$$\frac{dA}{dt} = -r_1 \cdot E_T \tag{5}$$

$$\frac{dB}{dt} = r_1 \cdot E_T - r_2 \cdot E_T \tag{6}$$

$$\frac{dC}{dt} = -r_2 \cdot E_T \tag{7}$$

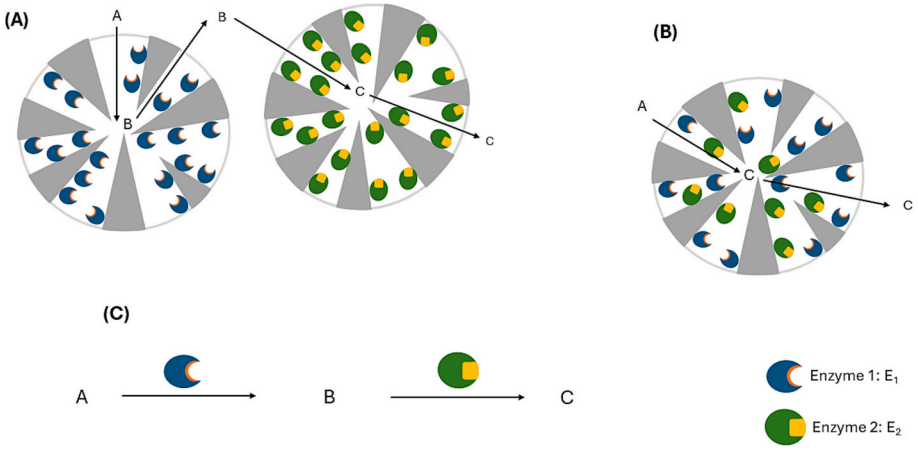

Fig. 1. Schematic representation of different combi-biocatalysts to be used in cascade reactions: **(A):** mixture of free enzymes; **(B):** mixture of individually immobilized enzymes and **(C):** co-immobilized enzymes.

The kinetic behavior is modulated by changing affinity constants K_M and the relative amount of E_1 and E_2 under the restriction of constant E_T.

2.1.2. Individually immobilized enzymes

In this case, each enzyme (*i*) is immobilized in a particle i where the reaction i takes place and the same kinetic expressions were used, but referred to the total volume of particle of each particle type (V_{Pi}) and the substrate *j* (A or B), thus:

$$r_i = \frac{kcat_i \cdot J}{K_{Mij} + J} \tag{8}$$

where r_i is the maximum specific reaction rate within each particle expressed as moles per unit of time and per unit of mass of enzyme i, $kcat_i$ are the catalytic kinetic constants in μmol min^{-1} mg^{-1}.

In all simulations, we assume that both enzymes are homogeneously distributed within the support matrix during immobilization. This assumption allows us to isolate the kinetic and diffusional effects without introducing spatial heterogeneity. The potential mass transfer effects were assessed by including a term for the substrate and product transport from the liquid bulk into the particle by using the maximum gradient model:

The transport terms are given by:

$$F_{ji} = K_L(J - J_i) \tag{9}$$

F_{ji} is the transport rate of component j (A, B or C) from the liquid bulk into the particle *i* (1 or 2) in units of moles per unit of time and unit of particle volume. K_L is a volumetric transport coefficient, *J* is the concentration of component j in the liquid bulk, and J_i is the concentration into the particle. The use of the maximum gradient model represents a simplified, global description of mass transport resistance and does not capture spatial concentration gradients within porous supports. However, it provides a simple and effective way to assess the influence of overall transport resistance on the performance of the system. In fact, the overall concentration difference ($J - Ji$) is a useful value for understanding the severity of diffusional limitations and the kinetic behavior of the immobilized enzyme.

For the balances of substrates and products, the transport and kinetic equations were coupled. Equation (10) expresses the variation of the concentration of component j inside the particle i due to reaction and transport from the bulk to the particle:

$$\frac{dJ_i}{dt} = R_j E_{iP} + F_{Ji} \tag{10}$$

where *Rj* is the reaction rate of *j* (positive for products, negative for substrates), E_{iP} is the concentration the enzyme i in the particle i.

Equation (11) expresses the variation of the concentration of component *j* in the liquid bulk:

$$\frac{dJ}{dt} = \sum -\frac{V_{pi}}{V_R} F_{Ji} \tag{11}$$

To focus the analysis on the relative amount of enzymes used (V_{pi}) and the ratio of affinity constants, it was imposed that the kinetic constant *k* is constant regardless of i, and E_i is constant irrespective of i. To facilitate data in-silico visualization, the following data has been used as basis for calculation: $kcat_1 = kcat_2 = 10$ μmol min^{-1} mg^{-1}, and $E_T = 1$ mg ml^{-1} and $E_{iP} = 100$ mg ml^{-1} and initial concentration of $A = 100$ mM. The ratio $V_{p1}/(V_{p1} + V_{p2})$ was used to study the effect of the relative variation of the two enzymes while keeping constant E_T.

Thus, to be able to compare the system with free enzymes the following restriction was made

$$\sum E_{iP} \cdot \frac{V_{pi}}{V_R} = E_T \tag{12}$$

2.1.3. Co-immobilized enzymes

In the co-immobilized enzyme system, both enzymes were immobilized within the same particle, allowing for potential enhancements in reaction efficiency due to compartmentalization and localized substrate effects. As previously, the kinetic expressions followed the Michaelis-Menten model, but in this case, the reaction rates (in terms of specific reaction rate expressed per unit of mass of enzyme) for reaction i (1 or 2) were expressed concerning the particle volume *Vp* and component j (A or B):

$$r_i = \frac{V_{maxi} \cdot J}{K_{Mij} + J} \tag{13}$$

Where:

$V_{maxi} = e_i k_{cati}$

r_i, V_{maxi} display units of specific reaction rate (per unit of mass of enzyme). *J* are the concentrations of the components A and B (in units of moles per unit of volume). *ei* represents the ratio between the enzyme concentration (E_{iP}) in the particle and the total enzyme concentration in the particle E_{TP}. $kcat_1$ and $kcat_2$ are the maximum specific activities.

In this configuration, substrate A diffuses into the co-immobilized enzyme particle and is converted to intermediate B by enzyme 1. The intermediate B is converted into product C by enzyme 2. Unlike the individually immobilized enzyme system, the transport between enzyme 1 and enzyme 2 occurs within the same particle.

Importantly, in all simulations, we assume that both enzymes are homogeneously distributed within the support matrix during co-immobilization. This assumption allows us to isolate the kinetic and diffusional effects without introducing spatial heterogeneity. The potential mass transport effects were assessed by including a term for the substrate and product transport from the liquid bulk into the particle by using the model of the maximum gradient.

The transport terms are given by:

$$F_{jp} = K_L(J - J_p) \tag{14}$$

F_{jp} is the transport rate of component j (A, B or C) from the liquid bulk into the particle *p* in units of moles per unit of time and unit of particle volume. Where K_L is a volumetric transport coefficient, *J* is the concentration of component *j* in the liquid bulk, and *Jp* is the concentration of component *J* inside the particle *p*. As in the previous case, the maximum gradient model offers a simplified, global view of mass transport resistance and does not capture spatial gradients within the support. However, it provides an effective way to assess how overall transport resistance impacts system performance. The total concentration difference ($J - Ji$) is a useful indicator of the severity of diffusional limitations and the kinetic behavior of co-immobilized enzymes.

For the balances of substrates and products, the transport and kinetic equations were coupled. Equation (15) expresses the variation of the concentration of component j inside the particle p due to reaction and transport from the bulk to the particle:

$$\frac{dJ_p}{dt} = R_j E_{TP} + F_{Jp} \tag{15}$$

where *Rj* is the reaction rate of j (positive for products, negative for substrates), and E_{TP} is the concentration of enzymes immobilized in the particle.

Equation (16) expresses the variation of the concentration of component *j* in the liquid bulk:

$$\frac{dJ}{dt} = -\frac{V_p}{V_R} F_{Ji} \tag{16}$$

where *Vp* is the total volume of particles, and *Vr* the reaction volume. To focus the analysis on the relative amount of the enzymes used (e1, e2), *kcati* was assumed to be constant irrespective of i. To facilitate data in-silico visualization, the following data has been used as basis for calculation: $kcat_1 = kcat_2 = 10$ μmol min^{-1} mg^{-1}, and $E_T = 1$ mg ml^{-1} and $E_{TP} = 100$ mg ml^{-1} and initial concentration of $A = 100$ mM. The ratio $e1 = E_{1P}/(E_{1P} + E_{2P})$ was used to study the effect of the relative

variation of the two enzymes while keeping constant E_T and E_{TP} constant.

Thus, to enable comparison with the system using free enzymes, the following restriction was imposed:

$$E_{TP}\frac{V_p}{V_R} = E_T \tag{17}$$

To compare different enzyme formulations, key efficiency parameters were computed:

Conversion of A (X_A):

$$X_A = \frac{A_0 - A}{A_0} \tag{18}$$

Yield of C formation:

$$Y_C = \frac{C}{A_0} \tag{19}$$

Average velocity of C formation:

$$R = \frac{C}{time} \tag{20}$$

Mass transport limitations were modulated by varying K_L (in the range of 6–2400), allowing a variation in the ratio between the characteristic times of reaction and transport, defined as:

$$t_{transport} = \frac{1}{K_L} \tag{21}$$

$$t_{reaction} = \frac{A_0}{R_J^* atA0} \tag{22}$$

Where R_J^* is the reaction velocity (in terms of moles per time and unit of reactor volume). The ratio of transport and reaction time was defined as a modified Thiele modulus, useful for assessing the magnitude of transport limitations:

$$\phi_{mod} = \frac{t_{transport}}{t_{reaction}} \tag{23}$$

Please note that in this study, the modified Thiele modulus was varied in the range from 10^{-3} to 1.1 to capture both kinetically controlled and diffusion-influenced regimes. While classical analysis considers $\Phi \gg 1$ necessary for strong diffusion limitation, our aim was to systematically investigate even low to moderate mass transfer resistance. This approach allows us to observe the early onset of the behavior, appreciable concentration gradients, and changes in effectiveness factor, all of which are relevant for understanding how kinetic asymmetry between enzymes impacts overall cascade performance.

Effectiveness factors were defined as:

$$\eta_A = \frac{-\frac{dA}{dt}}{r^*_{1atA}} \tag{24}$$

where the numerator expresses the observed decrease of the concentration of A in the liquid, and the denominator expresses the velocity (in terms of moles per time and unit of reactor volume) at the condition of the concentration of A in the liquid bulk.

$$\eta_{Cobs} = \frac{\frac{dC}{dt}}{r^*_{2atA}} \tag{25}$$

where the numerator expresses the observed increase of the concentration of C in the liquid, and the denominator expresses the velocity (in terms of moles per time and unit of reactor volume) at the condition most favorable for C production (initial concentration of A).

3. Results and discussion

3.1. Use of free enzymes

First, we investigated the optimization of the relative amounts of enzyme 1 and enzyme 2 for formulating an optimal combi-biocatalyst using free enzyme. The enzyme ratio is defined throughout as the proportion of enzyme 1 to the total enzyme amount. To systematically assess how enzyme kinetic properties affect cascade performance, we evaluated three representative scenarios with different ratios of K_M values for the two enzymes, under conditions where the initial substrate concentration to K_M ratio (A_0/K_M) was set to 2. This ensures the system operates in a mixed-order (0–1) kinetic regime, as discussed previously in the Methods section.

In this study, we evaluated enzyme formulation based on two distinct performance metrics. The first criterion is the initial reaction rate of product formation (*C*/time) measured at 20 % conversion of substrate A; this is the most widely used parameter for optimizing enzyme ratios due to its experimental convenience and sensitivity to formulation changes. The second criterion is the average productivity at a target yield, here defined as the rate of C formation (*C*/time) at 95 % yield—reflecting the practical goal of achieving high final conversion in industrial processes. By comparing the enzyme ratio that optimizes each criterion, we can directly observe how the choice of optimization metric influences the recommended biocatalyst composition.

The results of these simulations are summarized in Fig. 2, which shows the impact of enzyme ratio on both initial rate and productivity at high yield, for different K_M scenarios. The full reaction courses for each scenario are provided in Figs. S1–S3 (Supporting Information). In the case where the K_M values are identical for both enzymes, the curve of initial velocity of C production (when 20 % of the initial substrate has been consumed) using different ratios of the activities of both enzymes shifts towards a higher amount of enzyme 2. The enzymes ratio where the maximal initial velocity is obtained is 0.3. The situation is quite different when considering the maximum average rate at 95 % yield of C (the fixed final yield value set for the process) or the time required to reach this yield: the ratio between the amount of the two enzymes to achieve maximum activity and the shortest reaction time is 0.5. To reach 95 % yield, the reaction cycle must be around 70 min, following the conditions fixed in the model. The initial reaction rate under optimal conditions is 0.82, while the highest average reaction rate to reach 95 % yield is 1.34. This clearly exemplifies the importance of the lag time in the reaction, even with the slowdown of the reaction at values over 90 % (Fig. 3 shows optimal reaction cycles using the free enzymes), initial activity is lower than that required to reach 95 % C yield. Fig. 3 shows the reaction course under optimal enzyme mass ratio, the yield of B is higher than that of C until reaching a 30 %. The yield of C surpasses that of B after around 20 min of reaction. A is almost fully consumed when less than 5 % of B remains in the medium.

An important point is that the final “optimal” combi-biocatalyst defined using the initial reaction rates is quite far from the actual optimal one (the one that provides a shorter reaction time). This is because the increase in the percentage of enzyme 2 reduces the lag time, although it has later a negative effect on the global reaction rate. This combi-biocatalyst, with an enzymes ratio of 0.3, would require cycles of almost 91 min to reach 95 % conversion, almost 30 % longer than using a ratio of 0.5. Thus, relying on initial rates to define the optimal enzyme combination can lead to designing biocatalyst mixtures with sub-optimal properties.

When the K_{M2} was increased 10-fold (Fig. 2), the maximum initial rate was achieved using an enzyme ratio of 0.15 (i.e., a larger excess of enzyme 2 than in the previous case was required, significantly decreasing the amount of enzyme 1). This ratio was half that observed using enzymes with identical K_M values and also led to a slower production of C (the reaction rate now is 0.15). Again, the optimal ratio between the amount of both enzymes was different when considering

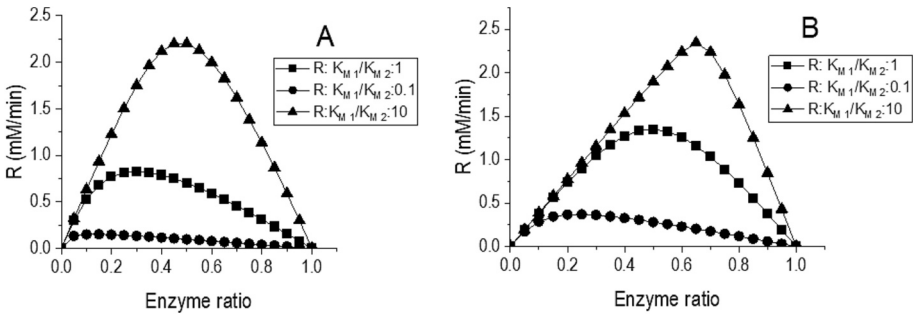

Fig. 2. Effect of the enzymes ratio (E_1/E_T) in the average rate of C formation (R, mM/min) using combi-biocatalysts with free enzymes (with different combinations of K_M values) under the condition of $A_0/K_{M1} = 2$: $K_{M1} = K_{M2} = 50$ (squares); mixtures of free enzymes with $K_{M1} = 50$ and $K_{M2} = 500$ (circles) and mixtures of free enzymes with $K_{M1} = 50$ and $K_{M2} = 5$ (triangles). **(A)**: At 20 % conversion of A and **(B)**: At 95 % yield of C. For further details see Methods section.

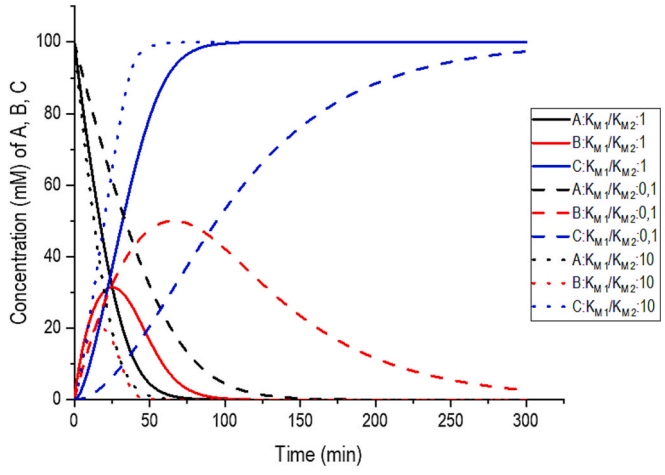

Fig. 3. Effect of the enzymes K_{M1} and K_{M2} in the reaction courses of the modification of A catalyzed by the respective optimal combi-biocatalysts prepared using mixtures of free enzymes to minimize the reaction time required to reach 95 % C yield (see Fig. 2) under the condition of $A_0/K_{M1} = 2$: $K_{M1} = K_{M2} = 50$ (solid line); $K_{M1} = 50$ and $K_{M2} = 500$ (dashed lines), $K_{M1} = 50$ and $K_{M2} = 5$ (dotted lines). Black lines: Substrate A; red lines: intermediate B and blue lines: product C. Additional parameters: $K_1 = K_2 = 10$, $E_T = 1$. Optimum E_1/E_T: ($K_{M1} = K_{M2} = 50$) = 0.5; ($K_{M1} = 50$ and $K_{M2} = 500$) = 0.25; ($K_{M1} = 50$ and $K_{M2} = 5$) = 0.65. (For interpretation of the references to colour in this figure legend, the reader is referred to the web version of this article.)

the average rate to produce 95 % product. The optimal ratio of enzymes was 0.25, meaning a 3-fold excess of enzyme 2 must be utilized to achieve the optimal value. Under these conditions, the average reaction rate was 0.37, more than 3.5-fold lower than when using enzymes with identical K_M values. This means that the reaction cycle must be increased to around 257 min to reach 95 % product. Moreover, it is also evident that using initial reaction rates to define the enzyme ratio may lead to a sub-optimal enzymes mixture. Using the enzymes mass ratio of 0.15 suggested by the mass ratio optimization using initial rates, the reaction time was prolonged to almost 277 min (7 % increase). However, the discrepancy was smaller than in the case of using enzymes with identical K_M values. The average reaction rate was almost 2.5 times higher than the maximum initial rate, showing the great relevance of the lag time in the initial rate. This is the reason that, using initial reaction activities to define the optimal enzyme ratio, to reduce the lag time is more important than the global reaction rate, meaning that a higher amount of enzyme 2 is apparently recommended. Again, the lag time was more relevant than the lowering of substrate A concentrations along the reaction. Fig. 3 shows the reaction course using the optimal enzymes mixture. In this case, the intermediate B is accumulated to a yield of 50 %, higher than when both enzymes presented similar K_M values, even using a higher excess of enzyme 2, and remains over the yield of C for around 100 min. A is fully consumed when a large percentage of B remains in the medium (more than 20 %).

When K_{M2} was 10-fold smaller than K_{M1} (Fig. 2), the picture changed radically. Using initial rates, the optimal biocatalyst mixture consisted of identical amounts of both enzymes. These initial rates were significantly higher than the optimal values in the other cases, surpassing the rates found using enzymes with identical K_M values by more than 2.5-fold. However, when considering the average rate or time required to reach 95 % product, the results were completely different. Now, an enzyme ratio of 0.65 gave the highest average rate and the shortest reaction time. In fact, the reaction time decreased to around 40 min compared to the use of enzymes with identical K_M values (requiring 1.73-fold shorter reaction cycles to reach the desired yield of the target product). Using the enzymes ratio defined by the optimal initial rates, the reaction time increased to 50 min (23 % increase). In this case, the lag time was shorter even using a smaller amount of enzyme 2 (as a result of the smaller K_M of enzyme 2, now the enzyme 2 is saturated at lower concentrations of B) (Fig. 3), meaning the initial rate was only 7 % lower than the activity derived from the average of the full reaction rate. From the reaction course using the optimal enzyme ratios (Fig. 3), it may be understood that even using an excess of enzyme 1, the maximum yield of B is around 20 %, and the yield of C surpasses that of B after around 5 min. The concentration of B is not above A at any point in the reaction.

These results clearly show the high relevance of the K_M values of the involved enzymes in determining the final optimal combi-biocatalyst for a cascade reaction, and how the evolution and maximum concentration of B differ in the different situations. When the K_M value of enzyme 2 is very high, a higher percentage of this enzyme is required to prepare the optimal biocatalyst, and the overall reaction time increases significantly. Conversely, if the K_M of this enzyme decreases, the reaction time decreases as well. Furthermore, the use of initial rates leads to sub-optimal enzyme mixtures. The percentage of enzyme 1 required to reach optimal reaction conditions is underestimated when using initial rates, as consequence of the significance of the enzyme 2 in reducing the lag time, critical for the initial rates but not so much for the global reaction rate.

3.2. *Use of individually immobilized enzymes*

To validate the model, a simulation was run with minimal mass transport limitations. This scenario resembles enzymes immobilized on very small porous particles or on the surface of a support, where diffusional effects are (almost) non-existent. It is expected that the results should be nearly identical to those obtained using free (soluble) enzymes. The results show that, indeed, in the near absence of diffusional limitations, the results were almost identical to those obtained with free enzymes (the figures show the case with enzymes having identical K_M), figure S4. An identical amount of both enzymes enabled to get the optimal results, but even under these minimal transport limitations, slight differences were observed compared to the free enzymes (initial

rates decreased from 0.82 to 0.79, and the time to reach 95 % yield increased from 70 to 74 min). In addition, the full reaction cycles using optimal enzymes ratio were very similar to the case of the combi-biocatalyst formed by free enzymes (Fig. S5). Using K_{M2} higher or lower than K_{M1}, similar results to the use of free enzymes were also observed (results not shown). Quantification of concentration gradients revealed that the differences between intraparticle and bulk concentrations for all species were negligible under these conditions (Fig. S5), confirming the absence of significant diffusional restrictions. This suggests that the model is functioning correctly. Based on this, we proceeded with introducing substrate and product diffusion limitations by increasing ϕ_{mod}. Figs. S6-S9 shows the different simulated reactions courses used.

Fig. 4 shows effects on the enzyme ratio. Fig. 5 shows the effects on the reaction time needed to reach 95 % of C yield under the optimal enzyme ratio. Under conditions of mass transport limitations, when the K_M values of both enzymes were identical (Fig. 4), an enzymes ratio of 0.20 (a 4-fold excess of enzyme 2) allowed the maximal initial rate. This value was slightly lower than the one observed with free enzymes (0.30). This additional increase in the enzyme 2 amount can be explained by the difficulties for the entry of B on the particle where the enzyme 2 is immobilized, the enzyme saturation will be lower than using free enzymes. The decrease in the maximal initial activity was more pronounced; the diffusional limitations of A and B led to a reduction in the observed reaction rate by 3.2-fold when comparing combi-biocatalysts formed by immobilized and free enzymes. However, when considering the average reaction rate or the time to reach 95 % yield, the optimal enzymes ratio was 0.5, similar to that observed with free enzymes. At this optimal enzymes ratio, the average rate was 1.6-fold higher than the optimal initial activity ratio, reflecting the importance of reducing the lag time in the initial rate of the system. This is interesting, considering that the lag time should have increased, but this effect was compensated by the slowing of the reaction due to mass transport limitations of the substrate A. In fact, the optimal reaction course now took 3.4-fold longer than when using free enzymes combi-biocatalyst. Of particular importance, in this case, is that using the optimal combi-biocatalyst composition derived from initial rates, the reaction course was almost 50 % longer than using the true optimal combination of enzymes. This difference was larger than when using free enzymes, with the cause being the larger underestimation of the amount of enzyme 1 when using the immobilized enzymes mixture. Fig. 5 shows the optimal reaction course. The accumulation of B is slightly higher than when using the combi-biocatalyst composed by free enzymes since the yield of B is higher than the yield of C until almost 80 % of A has been consumed.

Using enzyme 2 with a 10-fold increase in its K_M value (Fig. 4), the optimal enzymes ratio for the combi-biocatalyst using individually immobilized enzymes was the same as when using free enzymes, 0.15. The initial rate of this optimal combi-biocatalyst, formed by individually immobilized enzymes, was 0.1, approximately 2/3 of that found using

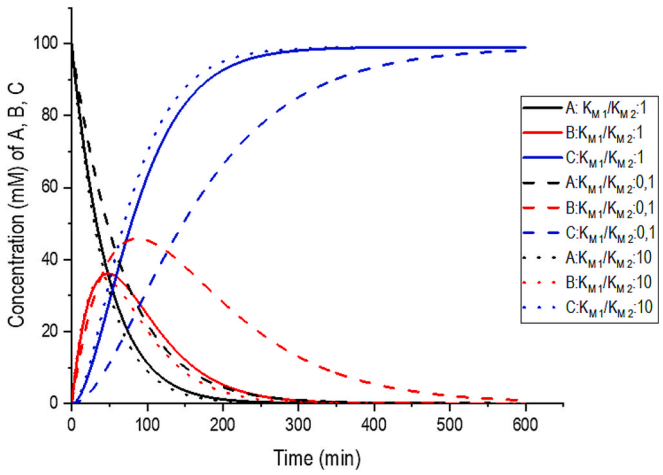

Fig. 5. Effect of the enzymes K_{M1} and K_{M2} in the reaction courses of the modification of A catalyzed by the respective optimal combi-biocatalysts prepared using individually immobilized enzymes with diffusional limitations to minimize the reaction time required to reach 95 % C yield under the condition of $A_0/K_M = 2$: $K_{M1} = K_{M2} = 50$ (solid line); $K_{M1} = 50$ and $K_{M2} = 500$ (dashed lines), $K_{M1} = 50$ and $K_{M2} = 5$ (dotted lines). Black lines: Substrate A; red lines: intermediate B and blue lines: product C. Additional parameters: $\phi_{mod} = 1.1$. Optimum V_{P1}/V_{Ptotal} ($K_{M1} = K_{M2} = 50$) = 0.65; ($K_{M1} = 50$ and $K_{M2} = 500$) = 0.35; ($K_{M1} = 50$ and $K_{M2} = 5$) = 0.55. η (effectiveness factor at 20 % conversion of A) ($K_{M1} = K_{M2} = 50$) = 0.38; ($K_{M1} = 50$ and $K_{M2} = 500$) = 0.58 and ($K_{M1} = 50$ and $K_{M2} = 5$) = 0.29; η (effectiveness factor at 95 % yield of C): ($K_{M1} = K_{M2} = 50$) = 0.31; ($K_{M1} = 50$ and $K_{M2} = 500$) = 0.59 and ($K_{M1} = 50$ and $K_{M2} = 5$) = 0.20. (For interpretation of the references to colour in this figure legend, the reader is referred to the web version of this article.)

similar free enzymes. This value was 2.5-fold lower than that found using the optimal combi-biocatalysts formed by immobilized enzymes with identical K_M values. Considering the global reaction course, the optimal ratio of both enzymes increased to 0.35, again remarking the great effect of the lag time in the initial reaction rate. The optimal average reaction rate more than doubled the initial activity value, again showing the relevance of the lag time in the initial rate. The optimal enzyme ratio was not the same as detected with free enzymes (which was 0.25). The reaction time using the optimal mixture of immobilized enzymes was 435 min. This was almost 1.7-fold longer than the time using the optimal combination of free enzymes and 1.9-fold slower than the optimal combi-biocatalysts formed by immobilized enzymes with identical K_M values. Using the combination of immobilized enzymes indicated by the optimal initial reaction rates, the reaction course was more than 37 % longer than using the actual optimal combi-biocatalyst. The reaction course can be visualized in Fig. 5. In this instance, the maximum yield of B was around 45 %, higher than using the free enzymes and remained higher than C even when only 10 % A remains in

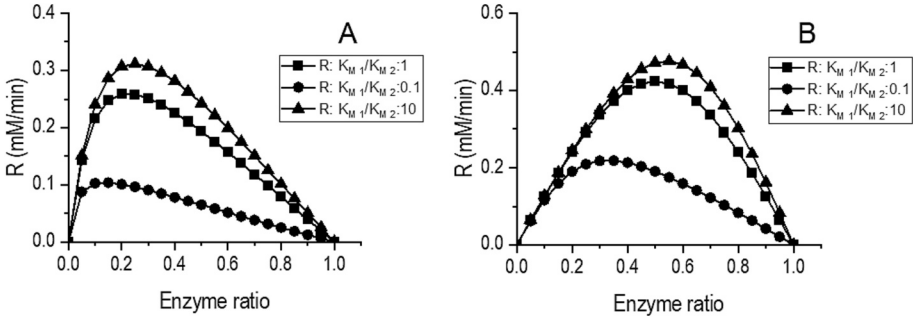

Fig. 4. Effect of the enzyme ratio (V_{P1}/V_{Ptotal}) in the average rate of C formation (R, mM/min) using individually immobilized enzymes with diffusional limitations and different combinations of K_M values under the condition of $A_0/K_{M1} = 2$: ($K_{M1} = K_{M2} = 50$): solid squares; ($K_{M1} = 50$ and $K_{M2} = 500$): solid circles and ($K_{M1} = 50$ and $K_{M2} = 5$): solid triangles. **(A)**: At 20 % conversion of A and **(B)**: At 95 % yield of C. Additional parameters: $\phi_{mod} = 1.1$.

the reaction (Fig. 5). A is fully consumed when a large amount of B is still present in the reaction medium.

Finally, Fig. 4 shows the case where the K_{M2} is 10-fold lower. Using the initial rates in the optimization of the enzymes ratio, the optimal enzyme combination was 0.25 (which is quite different from the use of free enzymes, increasing the amount of enzyme 2). The value of this optimal initial rate reached using the combi-biocatalyst formed by immobilized enzymes is greatly decreased compared to the value observed using the optimal combi-biocatalyst composed by similar free enzymes, by more than 7-fold. However, this value was almost 25 % higher than when using the optimal combi-biocatalyst formed by immobilized enzymes with identical K_M values. For the global reaction, the optimal enzymes ratio became 0.55, meaning that more immobilized enzyme 2 was required to reach the optimal value compared to the case of combi-biocatalyst formed by free enzymes (enzymes ratio 0.65). The optimal average rate of the reaction with this combi-biocatalyst was around 50 % higher than the initial optimal rate, again showing the high relevance of the lag time in the initial rate and the lower impact in the average global reaction rate. The time to reach 95 % yield was 199.62 min, very similar to the optimal reaction cycle using optimal mixture of immobilized enzymes with identical K_M values, but almost 5-fold slower than when using optimal mixture of similar free enzymes. Fig. 5 shows the reaction course with the optimal combi-biocatalyst composed of immobilized enzymes, a certain lag time is visible, and the yield of B surpassed the yield of C until around 70 % of A has been consumed. A and B a yields become similar when around 70 % A has been consumed, and all A is consumed when only around 5 % of B remains in the reaction medium.

The results presented here indicate some clear facts:

i. The optimal combination of enzymes calculated using free enzymes did not match that combination determined using immobilized enzymes when mass transport limitations were considered, even assuming that immobilization did not alter the kinetic properties of the enzymes.
ii. As in the case of the combi-biocatalyst composed by free enzymes, the percentage of enzyme 1 required to reach the optimal reaction conditions was underestimated when using initial rates to determine the optimal enzyme ratio. The performance of the optimal combi-biocatalyst designed using initial rates is far from that of the real optimal biocatalyst calculated using the global reaction course.
iii. Substrate and product mass transport limitations significantly decrease the global reaction rate when using individually immobilized enzymes. The influence of mass transport limitations can also be observed in the decrease of the effectiveness factor and the generation of concentration gradients between the particle and the bulk phase (Fig. S10). While the concentration gradients for substrate A remain similar regardless of the K_M ratio, an increase in the K_{M1}/K_{M2} ratio is associated with a pronounced increase in the observed concentration gradient for the intermediate (Fig. S10). This highlights how diffusional resistance and kinetic asymmetry together exacerbate concentration gradients within the system. Although most simulated Φ values correspond to weak or moderate diffusional limitations according to classical criteria, our results show that significant substrate and intermediate gradients—and reductions in effectiveness factor—can still arise. This transitional regime, where neither purely kinetic nor extreme diffusion control dominates, is particularly valuable for exploring the interplay between enzyme kinetic asymmetry and mass transport, as addressed in this study.
iv. K_{M2} plays a critical role in the use of enzyme mixtures. K_{M2} similar to or smaller than K_{M1} can lead to a significant improvement in the performance of this kind of combi-biocatalyst.

3.3. Use of co-immobilized enzymes

As explained in the introduction, most authors assume that the use of co-immobilized enzymes must exert a very significant improvement on their global performance in a cascade. Here we will analyze this for different K_M values for the enzymes as explained above.

Initially, the effect of co-immobilizing enzymes in almost full absence of mass transport limitations is presented in Figs. S4 and S5 for the case where the K_M of both enzymes is identical in the combi-biocatalyst formed by co-immobilized enzymes. The figure shows as expected that the performance in this case is almost identical to combi-biocatalysts composed by mixtures of free enzymes or mixtures of immobilized enzymes in absence of diffusional limitations. When K_{M2} is higher or lower than K_{M1}, values were also similar to the use of free enzymes (not showed results). Quantification of concentration gradients under these conditions showed negligible differences between intra-particle and bulk concentrations for each species (Fig. S5), confirming that mass transport was not limiting. In this way, we can validate that there are no model artefacts. Figs. S11-S14 shows the different simulated reactions courses used.

Fig. 6 shows effects on the enzyme ratio. Fig. 7 shows the effects on the reaction time needed to reach 95 % of C yield under the optimal enzyme ratio. Regarding the condition using co-immobilized enzymes with identical K_M and mass transport limitations, the results are dissimilar to the use of the mixtures of free enzymes using initial reaction rates, now the curve “initial reaction rate” versus “different ratios of the co-immobilized enzymes” is fully symmetric, maximum initial activity is achieved using identical amounts of both enzymes in the co-immobilized combi-biocatalyst (i.e. a ratio of 0.5). The maximum initial rate is 1.395. This value is 1.7-fold higher than the results obtained using blends of free enzymes. That is, assuming that there are not negative effects on the enzymes performance caused by the immobilization, the initial production rate of the target compound is higher using optimal co-immobilized enzymes than using the optimal mixtures of free enzymes, mass transport limitations of the product inside the co-immobilized biocatalyst cause a higher efficiency of the second enzyme and lead to higher initial reaction rates. More significant, this value is 5.36-fold higher than using the optimal blend of enzymes independently immobilized. Using the global reaction, the optimal co-immobilized combi-biocatalyst also have an optimal enzymes ratio of 0.5. A first remarkable fact is that, using co-immobilized enzymes, the initial rates are higher than the average reaction rates (almost by 2-fold) in contrast to all the previous cases. This is due to a significant decrease of the lag time (Fig. 7) in the reaction. However, the global reaction rate is lower than when using the combi-biocatalyst formed by the mixture of free enzymes and the reaction cycle is longer (by 1.7-fold), resulting from the decrease in the activity of enzyme 1 due to mass transport limitations, effect that increased when the concentration of the A decreases during the reaction. That means that even although the initial reaction rates were higher using the co-immobilized enzymes, the time to reach the target yield is longer than when using the mixture free enzymes. That is, the co-immobilized enzymes are less efficient than the combi-biocatalyst formed by free enzymes considering the global reaction. However, the optimal co-immobilized combi-biocatalyst was more than 1.8-fold more efficient in the global reaction than the optimal mixture of enzymes immobilized in an individual form. This 1.8-fold increase is the real gain achieved by the co-immobilization, not the more than 5-fold highlighted using initial rates. In this case, the optimal ratio of both enzymes is the same using initial rates or global reaction parameters. It is also the same using the free or the individually immobilized. Fig. 7 shows the reaction course using the co-immobilized combi-biocatalyst prepared using the optimal enzymes ratio where the evolution of the yields of B can be observed. In contrast to the results using combi-biocatalyst formed by the free enzymes or the independently immobilized enzymes, the yield of B is not above the yield of C at any point, the yields of B hardly reaching 15 % as a consequence of its

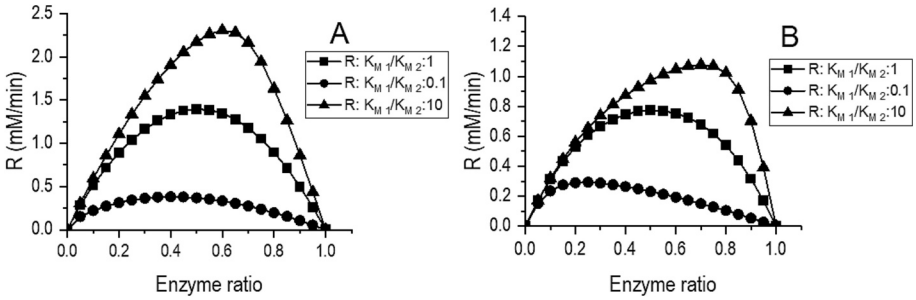

Fig. 6. Effect of the enzyme ratio (E_{1P}/E_{TP}) in the average rate of C formation (R, mM/min) using co-immobilized enzymes with diffusional limitations and different combinations of K_M values under the condition of $A_0/K_{M1} = 2$: ($K_{M1} = K_{M2} = 50$): solid squares; ($K_{M1} = 50$ and $K_{M2} = 500$): solid circles and ($K_{M1} = 50$ and $K_{M2} = 5$): solid triangles. **(A)**: At 20 % conversion of A and **(B)**: At 95 % yield of C. Additional parameters: $\phi_{mod} = 1.1$.

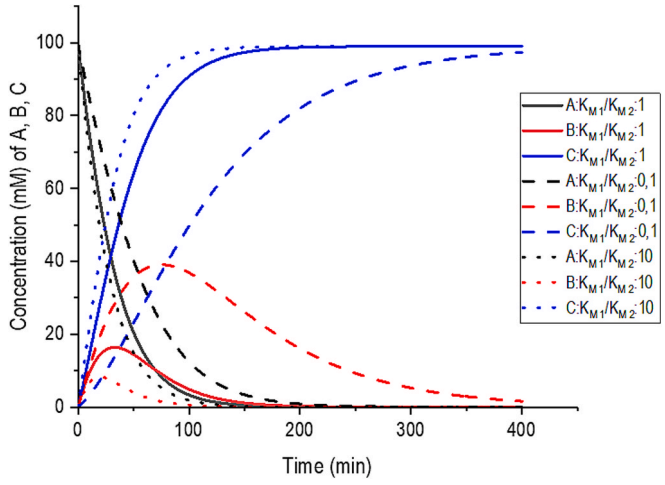

Fig. 7. Effect of the enzymes K_{M1} and K_{M2} in the reaction courses of the modification of A catalyzed by the respective optimal combi-biocatalysts prepared using co-immobilized enzymes with diffusional limitations to minimize the reaction time required to reach 95 % C yield under the condition of $A_0/K_{M1} = 2$: $K_{M1} = K_{M2} = 50$ (solid line); $K_{M1} = 50$ and $K_{M2} = 500$ (dashed lines), $K_{M1} = 50$ and $K_{M2} = 5$ (dotted lines). Black lines: Substrate A; red lines: intermediate B and blue lines: product C. Additional parameters: $\phi_{mod} = 1.1$. Optimum V_{P1}/V_{Ptotal} ($K_{M1} = K_{M2} = 50$) = 0.5; ($K_{M1} = 50$ and $K_{M2} = 500$) = 0.25; ($K_{M1} = 50$ and $K_{M2} = 5$) = 0.7. η (effectiveness factor at 20 % conversion of A) ($K_{M1} = K_{M2} = 50$) = 1.29; ($K_{M1} = 50$ and $K_{M2} = 500$) = 2.19 and ($K_{M1} = 50$ and $K_{M2} = 5$) = 0.87; η (effectiveness factor at 95 % yield of C): ($K_{M1} = K_{M2} = 50$) = 0.57; ($K_{M1} = 50$ and $K_{M2} = 500$) = 0.79 and ($K_{M1} = 50$ and $K_{M2} = 5$) = 0.46. (For interpretation of the references to colour in this figure legend, the reader is referred to the web version of this article.)

rapid transformation to C. The yield of B is slightly above A remaining in the medium when A is less than 10 %, but when A is fully consumed, almost no B can be found, unlike the reaction using the free enzymes (Fig. 3) or the individually immobilized enzymes (Fig. 5).

When the K_{M2} was increased 10-fold, Fig. 6 shows the results. The maximal initial reaction rate is obtained with co-immobilized enzymes at an enzymes ratio of 0.4, an excess of enzyme 2 is necessary to compensate for higher K_M compared to the previous case. Compared to the free enzymes, where the enzymes ratio in the optimal combi-biocatalyst is 0.1 using the initial activities to determine the optimal combination of enzymes, it is evidently a very different situation. Moreover, the optimal initial activity of the co-immobilized enzymes is 2.7 higher than that using the blend of free enzymes, very likely due to the smaller amount of enzyme 1 using the free enzymes. This improved optimal initial rate of the combi-biocatalyst, it becomes over 3.5-fold higher compared to the mixture of individually immobilized enzymes. However, using the full reaction cycle, the optimal ratio of enzymes is 0.25 for the co-immobilized enzymes, as the value using the free enzymes, and with more enzyme 2 than using the individually immobilized enzymes (where the optimal ratio is 0.35). Using the optimal co-immobilized enzymes, the reaction took more than 1.25-fold longer than using the optimal combi-biocatalysts prepared using free enzymes (due to the mass transport limitations of A), but 1.33-fold shorter time than using the enzymes immobilized in an individual form. Again, using the initial rates, it appears that co-immobilized enzymes are more efficient than the mixture of the free enzymes, but it is just the consequence of avoiding the lag time (Fig. 7). However, optimal mixture of free enzymes performs the reaction in a shorter time compared to the optimal co-immobilized enzymes, as the mass transfer limitations of A reduce the activity of enzyme 1 in the co-immobilized biocatalyst. Curiously, the gain of the enzymes co-immobilization is shorter now than when the K_M of both enzymes is identical.

Using the optimal enzymes ratio value calculated using initial rates to prepare the co-immobilized combi-biocatalyst, the reaction course will be 10 % slower than using the actual optimal co-immobilized combi-biocatalyst. If we extrapolate the optimal enzymes ratio calculated using the global performance of the blend of individually immobilized enzymes to prepare the co-immobilized enzymes, the reaction takes 24 % longer that using the actual optimal combi-biocatalyst. The advantage of co-immobilization almost disappears. Using the mixture of free enzymes, the optimal enzymes ratio is the same than using co-immobilized enzymes. The reaction course (Fig. 7) shows a lower accumulation of B (maximum B yields are under 40 %) compared to the use of free or independent immobilized enzymes with this K_M combination, that is consumed faster now.

Fig. 6 shows the results when K_{M2} is 10-fold lower than K_{M1}. The maximum initial rate is achieved at an enzymes ratio of 0.4, slightly lower than using optimal combi-biocatalyst of the free enzymes (0.5), and higher than using mixtures of the independently immobilized enzymes (0.25). The maximum activity was 0.38, much lower than using the optimal blend of free enzymes but more than 22 % faster than the optimal combi-biocatalyst formed by the independently immobilized enzymes.

Using the global reaction, the optimal combination of both enzymes in the co-immobilized combi-biocatalyst was at a ratio of 0.7, an excess of enzyme 1 must be utilized to maximize the activity of the co-immobilized enzymes combi-biocatalyst. Using the mixtures of free enzymes, this ratio was 0.65, it was 0.55 using the combination of individually immobilized enzymes. This suggests that, as expected, when the importance of the lag time decrease, a higher amount of enzyme 1 gives the highest activities in the co-immobilized combi-biocatalyst. The initial rate was almost twice that of the global activity, showing the almost full disappearance of the lag time influence in the initial rate. The global reaction rate was more than 2.4-fold higher than using the mixture of the individually immobilized enzymes but it was around 2.2-fold lower than using the blend of free enzymes. Fig. 7 shows the reaction course using the optimal co-immobilized combi-biocatalyst, where maximum B yield is the lowest of all the studied systems and

never is higher than the yields of C, even it is lower than the remaining percentage of A until the end of the reaction.

In this way, this K_M ratio is the situation where the used of co-immobilized enzymes is more advantageous from a kinetic point of view compared to the use of mixtures of individually immobilized enzymes. If the enzyme ratios are extrapolated from the data obtained using the optimal mixture of free enzymes, the global reaction time only increases from 88 to 89 min, but using the optimal enzymes ratio calculated utilizing the combination of individually immobilized enzymes, this value increases to 93 min. Differences are not very large, but still a 5 % time may be saved with a proper optimization of the co-immobilized enzymes design.

Hence, the results presented in this section show some clear points, Figs. 8 and 9 summarize the main results of this paper, Figs. S15-S18 show the time courses associated to the summary Figures.

i. Using initial reaction rates, it appears that the co-immobilized enzymes become more efficient that the mixture of free enzymes but this is not a real situation considering the full reaction cycle.
ii. .- The apparent advantage of using co-immobilized enzymes versus combinations of individually immobilized enzymes is much higher using initial activity ratios that the real one, considering global reaction courses.
iii. – Substrate mass transport limitations decrease the overall reaction rate, though this effect is less pronounced than when using individually immobilized enzymes. The impact of mass transport resistance is also evident in the smaller reduction of the effectiveness factor and the development of concentration gradients between the particle and the bulk phase (Fig. S19). The concentration gradients for substrate A are similar regardless of the K_M ratio, and the gradient for intermediate B remains nearly negligible under these conditions (Fig. S19). During the lag phase (initial reaction rate) the concentration of intraparticle B is higher than in the bulk supporting the fact the initial formation rate of C provided by the coimmobilized enzymes is higher than free enzyme.
iv. .- The use of co-immobilized biocatalyst with an enzyme 2 having a much higher K_M is the only case where the percentage of enzyme 1 is over estimated if the optimal enzyme ratios are calculated using initial rates and not the whole reaction course (including combi-biocatalysts formed by free or individually immobilized enzymes). This includes the 9 cases studied in this paper.
v. .- Optimal ratio of enzymes for the preparation of the co-immobilized biocatalyst can be nearly extrapolated from the results using the optimal mixtures of free enzymes even if they are not exact. Results are identical if the K_M values are similar or K_{M2} is higher than K_{M1}. If the K_{M2} is lower than K_{M1}, there are some differences, but the effects on the time necessary to complete one reaction cycle are not very significant.

4. Overall discussion and conclusions

The results presented in this paper show some relevant factors using several enzymes in multi-enzymatic cascades. Figs. 8 and 9 offer a summary of the most relevant results. Optimal enzyme ratio dependent on enzyme formulation, kinetic parameters and mass transport control are shown in Fig. 8. the reaction time needed to reach the target of 95 % of C formation yield is plotted as a function of biocatalyst formulation, kinetic constants and mass transport control at the optimal enzyme ratio. The first fact is that the use of enzymes where K_{M2} is similar to or lower than K_{M1} may be very relevant to have mixtures of enzymes with very good performance. This may have more impact in the final combi-biocatalysts performance than a proper design of the final combination of enzymes or the use of co-immobilized enzymes. If possible, a very high K_{M2} should be avoided.

The substrate A mass transfer limitations produce a severe decrease in the cascade reaction rate. These diffusional problems can explain a worsening of the reaction rate even if the enzyme properties are fully preserved, as in the current presentation. The diffusional problems (in this instance of the intermediate B) are responsible for an increase in the initial reaction rate using co-immobilized enzymes. This way, apparent super-activation of the co-immobilized enzymes compared to mixtures

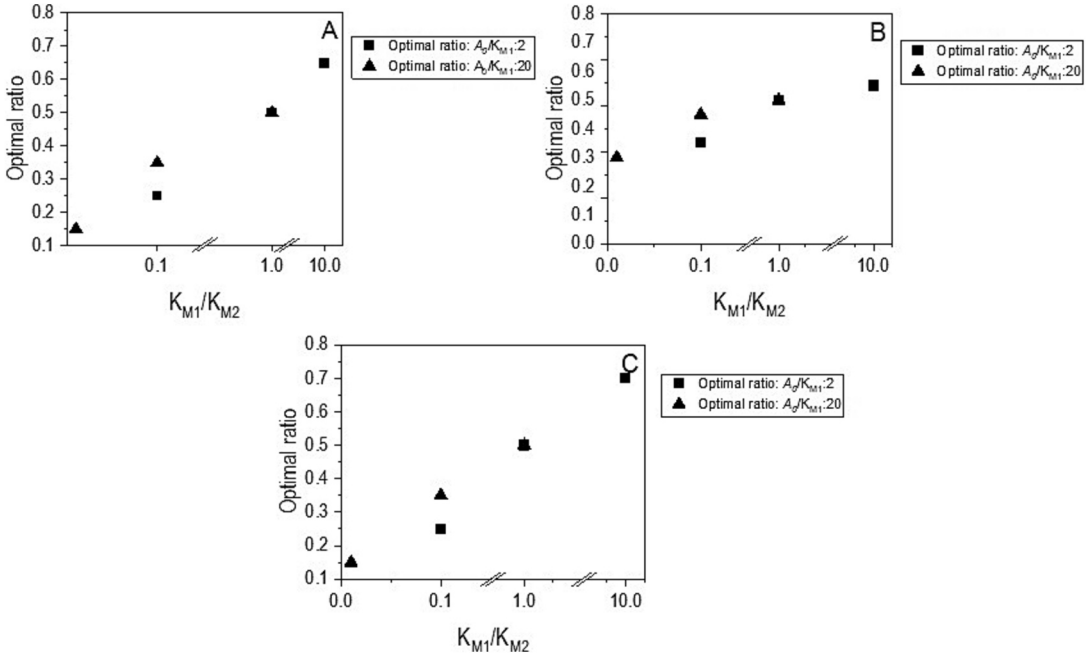

Fig. 8. Effect of different the K_{M1}/K_{M2} on the optimal enzyme ratio to obtain a 95 % yield of C by the respective optimal combi-biocatalysts prepared using free enzymes **(A)**; individually immobilized enzymes **(B)** and co-immobilized enzymes **(C)**. Fig. 9**:** Time required to obtain a 95 % yield of C at different K_{M1}/K_{M2} by the respective optimal combi-biocatalysts prepared using free enzymes **(A)**; individually immobilized enzymes **(B)** and co-immobilized enzymes **(C)**.

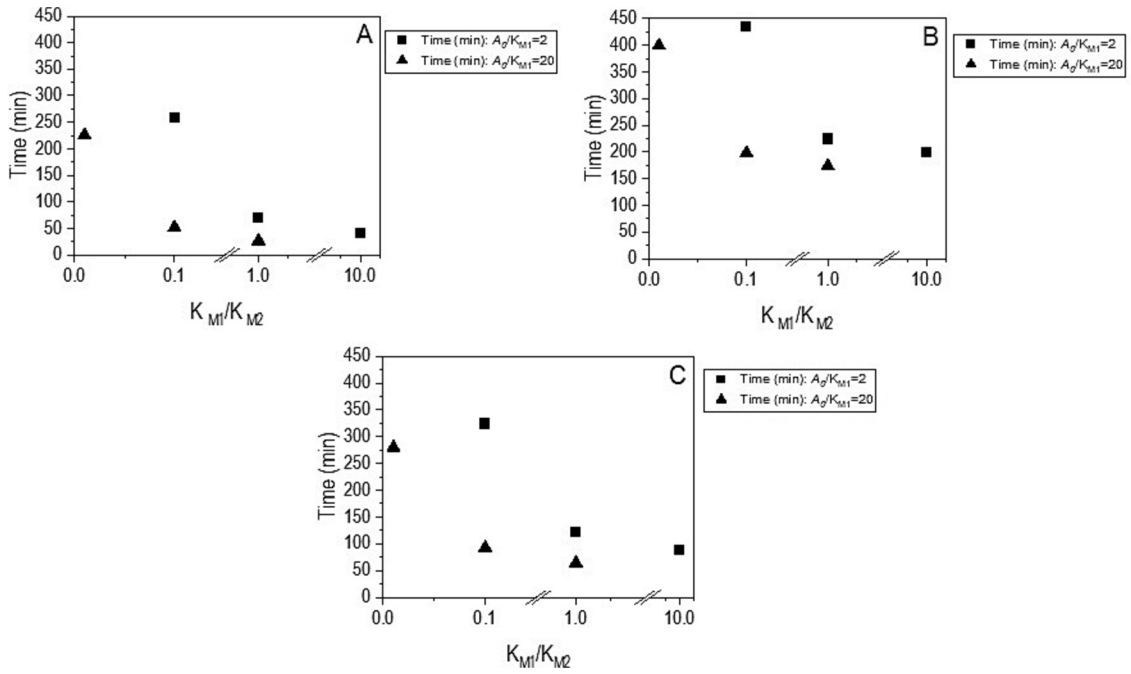

Fig. 9. Time required to obtain a 95 % yield of C at different K_{M1}/K_{M2} by the respective optimal combi-biocatalysts prepared using free enzymes **(A)**; individually immobilized enzymes **(B)** and co-immobilized enzymes **(C)**.

of free enzymes can be expected when co-immobilizing enzymes if measuring the formation of the final product, as in the first moments of the reaction, the lag time produced by the lack of intermediate product means that the final product cannot be synthesized in other combinations of enzymes. However, this is not translated to the global reaction. In fact, the global reaction catalyzed by the co-immobilized enzymes is slower than that catalyzed by the mixture of the free enzymes, as a consequence of the mass transfer of A.

The results also show that, in most instances, the use of initial rates to define the ratio of enzymes may lead to a sub-optimal combi-biocatalyst giving as a result an excess of enzyme 2 (to decrease the lag time). The optimization of the combination of enzymes must be performed using the time necessary to reach the desired reaction yield. This is true mainly using the free and individually immobilized enzymes. Using co-immobilized enzymes, the composition of the optimal biocatalyst is similar using the data from the full reaction course or initial reaction rates only in the case of enzymes with similar K_M. Other instances give an excess of the enzyme with the higher K_M in the final co-immobilized combi-biocatalyst if using the initial reaction rates.

The extrapolation of the results using the optimal mixture of free enzymes are not valid to define the optimal ratio of enzymes using individually immobilized enzymes, but, curiously, they may be valid to design the co-immobilized enzymes combi-biocatalyst. The optimal combi-biocatalyst compositions are identical when the K_M of both enzymes were identical or if K_{M2} is higher than K_{M1}, and similar if K_{M2} is lower. However, this is not true if the optimization of the enzymes composition for the co-immobilized combi-biocatalyst is performed using the values obtained when using the mixtures of immobilized enzymes, except if the enzymes have identical K_M.

That way, with information on the K_M values of the enzymes involved in the process, it is possible to decide if it is possible to use or not the values calculated using free enzyme mixtures or initial rates. If the immobilization induces changes in the kinetic properties of the enzymes, or if the products have some inhibition potential in enzyme 1 or 2 (a more realistic system), the system optimization will be more complex.

To validate our modeling framework under conditions of higher A_0/K_M, we have included in Figs. 8 and 9 the equivalent cases for the condition of $A_0/K_M = 20$, where zero order kinetic applied to the reaction (1) (The corresponding time courses are included as Fig. S20-21). Similar trends and conclusions applied and are observed but reaction times are lower for all the biocatalyst formulations.

The use of identical k_{cat} values and the exclusion of enzyme inhibition and deactivation were deliberate simplifications in this study. While these assumptions allowed us to focus on kinetic asymmetry (through K_M) and mass transport limitations, they necessarily constrain the generality of our model. In practical applications, differences in kcat between enzymes can shift the rate-determining step in a cascade and thereby alter the optimal enzyme ratio. For example, if E2 has a much lower turnover number than E1, a higher E2 loading would be required, regardless of K_M values. Similarly, differences in enzyme stability can affect catalyst lifetime and process economics, and may render co-immobilization undesirable if one enzyme deactivates more rapidly than the other. Incorporating these additional factors into future modeling efforts would provide a more comprehensive basis for biocatalyst optimization.. In summary, these results indicate significant differences in effective use of the two enzymes, dependent upon the ratio in which they are added (for the three type of formulation biocatalysts). This is of great importance for the process operation, but also to incorporate in the design of combi-biocatalysts. Further complications can clearly arise when one enzyme is much for stable than the other. However, what is also clear from the results presented here is that the effect of the individual enzyme K_M values is also of great significance. This is to be expected, but the work here also provides a quantitative indication about the effect of lowering of K_M values for a given enzyme and the return that may be granted. Protein engineering allows the modification of K_M values, although K_{cat}/K_M is still too often used as the metric for screening. In principle, enzymes can be engineered and screened for lower K_M values (Woodley 2022). Using the data from this paper the cost-benefit analysis of making such protein changes can now be evaluated.

In this study, we have advanced the understanding of the design of immobilized multi-enzymatic systems in a novel but complementary manner to previous approaches. (Høst et al., 2022; Paschalidis et al., 2023; (Paschalidis et al., 2024)). We evaluated enzyme formulation using two distinct performance metrics: initial activity and final product yield. This binary treatment highlights how the choice of optimization

criterion can influence design outcomes. However, industrial biocatalyst development often requires balancing multiple objectives—such as maximizing productivity, minimizing enzyme cost, and achieving full conversion within a defined time frame. Incorporating multi-objective optimization frameworks could significantly enhance the practical utility of this modeling approach (Paschalidis et al., 2022). Such frameworks would enable simultaneous evaluation of trade-offs, thereby guiding the selection of enzyme ratios or formats that best meet a broader set of process constraints. We see this as a valuable direction for future work.

Finally, while our model employs a lumped parameter approach (via K_L) to describe mass transfer limitations, this choice prioritizes simplicity and computational efficiency over spatial accuracy. It allows us to explore broad trends and perform dynamic, system-level optimization across many kinetic regimes. However, these simplifications also limit our ability to capture intraparticle concentration gradients, local enzyme saturation, or heterogeneity in enzyme positioning within supports. More mechanistic, spatially resolved models have been proposed (e.g., (Paschalidis et al., 2023)) which can capture local concentration gradients and enzyme positioning effects in porous carriers and derive analytical criteria for optimal enzyme arrangements. These fine-grained spatial models complement our lumped dynamic framework, and a hybrid approach incorporating both spatial and temporal dynamics could further improve the predictive power and applicability of in silico biocatalyst design.

CRediT authorship contribution statement

Diego Carballares: Writing – review & editing, Writing – original draft, Visualization, Software, Methodology, Investigation. **John M. Woodley:** Writing – review & editing, Writing – original draft, Visualization, Investigation, Conceptualization. **Roberto Fernandez-Lafuente:** Writing – review & editing, Writing – original draft, Visualization, Supervision, Resources, Project administration, Methodology, Investigation, Funding acquisition, Formal analysis, Data curation, Conceptualization. **Juan M. Bolivar:** Writing – review & editing, Writing – original draft, Visualization, Validation, Supervision, Software, Resources, Project administration, Methodology, Investigation, Funding acquisition, Formal analysis, Data curation, Conceptualization.

Declaration of competing interest

The authors declare that they have no known competing financial interests or personal relationships that could have appeared to influence the work reported in this paper.

Acknowledgments

Dr. Fernandez-Lafuente gratefully recognizes the financial support from Ministerio de Ciencia e Innovación-Spanish Government (project PID2022-136535OB-I00.) JMB acknowledges funding from project CNS2022-135541 financed by MICIU/AEI /10.13039/501100011033 and by European Union NextGeneration EU/PRTR. DCN and JMB ackowledges funding from Pathfinder Open 2022, a European Innovation Council (EIC) work program that is part of Horizon Europe (grant agreement no. 101099528) and UK Innovation Funding Agency (UKRI) (reference no. 10062709).

Appendix A. Supplementary data

Supplementary data to this article can be found online at https://doi.org/10.1016/j.ces.2025.122219.

Data availability

Data will be made available on request.

References

Alonso, S., Santiago, G., Cea-Rama, I., Fernandez-Lopez, L., Coscolín, C., Modregger, J., Ressmann, A.K., Martínez-Martínez, M., Marrero, H., Bargiela, R., Pita, M., Gonzalez-Alfonso, J.L., Briand, M.L., Rojo, D., Barbas, C., Plou, F.J., Golyshin, P.N., Shahgaldian, P., Sanz-Aparicio, J., Guallar, V., Ferrer, M., 2020. Genetically engineered proteins with two active sites for enhanced biocatalysis and synergistic chemo- and biocatalysis. Nat. Catal. 3, 319–328. https://doi.org/10.1038/s41929-019-0394-4.

Arana-Peña, S., Carballares, D., Morellon-Sterling, R., Rocha-Martin, J., Fernandez-Lafuente, R., 2022. The combination of covalent and ionic exchange immobilizations enables the coimmobilization on vinyl sulfone activated supports and the reuse of the most stable immobilized enzyme. Int. J. Biol. Macromol. 199, 51–60. https://doi.org/10.1016/j.ijbiomac.2021.12.148.

Arana-Peña, S., Carballares, D., Morellon-Sterlling, R., Berenguer-Murcia, Á., Alcántara, A.R., Rodrigues, R.C., Fernandez-Lafuente, R., 2021. Enzyme co-immobilization: always the biocatalyst designers' choice…or not? Biotechnol. Adv. 51, 107584. https://doi.org/10.1016/j.biotechadv.2020.107584.

Arnold, F.H., 2018. Directed evolution: Bringing new chemistry to life. Angew. Chemie Int. Ed. 57, 4143–4148. https://doi.org/10.1002/anie.201708408.

Barbosa, O., Ortiz, C., Berenguer-Murcia, Á., Torres, R., Rodrigues, R.C., Fernandez-Lafuente, R., 2015. Strategies for the one-step immobilization-purification of enzymes as industrial biocatalysts. Biotechnol. Adv. 33, 435–456. https://doi.org/10.1016/j.biotechadv.2015.03.006.

Bernal, C., Rodríguez, K., Martínez, R., 2018. Integrating enzyme immobilization and protein engineering: an alternative path for the development of novel and improved industrial biocatalysts. Biotechnol. Adv. 36, 1470–1480. https://doi.org/10.1016/j.biotechadv.2018.06.002.

Bilal, M., Asgher, M., Cheng, H., Yan, Y., Iqbal, H.M.N., 2019a. Multi-point enzyme immobilization, surface chemistry, and novel platforms: a paradigm shift in biocatalyst design. Crit. Rev. Biotechnol. 39, 202–219. https://doi.org/10.1080/07388551.2018.1531822.

Bilal, M., Zhao, Y., Noreen, S., Shah, S.Z.H., Bharagava, R.N., Iqbal, H.M.N., 2019b. Modifying bio-catalytic properties of enzymes for efficient biocatalysis: a review from immobilization strategies viewpoint. Biocatal. Biotransform. 37, 159–182. https://doi.org/10.1080/10242422.2018.1564744.

Bolivar, J.M., Woodley, J.M., Fernandez-Lafuente, R., 2022. Is enzyme immobilization a mature discipline? some critical considerations to capitalize on the benefits of immobilization. Chem. Soc. Rev. 51, 6251–6290. https://doi.org/10.1039/D2CS00083K.

Bornscheuer, U.T., Pohl, M., 2001. Improved biocatalysts by directed evolution and rational protein design. Curr. Opin. Chem. Biol. 5, 137–143. https://doi.org/10.1016/S1367-5931(00)00182-4.

Butò, S., Pollegioni, L., D'Angiuro, L., Pilone, M.S., 1994. Evaluation of D -amino acid oxidase from *Rhodotorula gracilis* for the production of α-keto acids: a reactor system. Biotechnol. Bioeng. 44, 1288–1294. https://doi.org/10.1002/bit.260441104.

Carballares, D., Morellon-Sterling, R., Fernandez-Lafuente, R., 2022a. Design of artificial enzymes bearing several active centers: new trends, opportunities and problems. Int. J. Mol. Sci. 23, 5304. https://doi.org/10.3390/ijms23105304.

Carballares, D., Rocha-Martin, J., Fernandez-Lafuente, R., 2022b. Chemical amination of immobilized enzymes for enzyme coimmobilization: Reuse of the most stable immobilized and modified enzyme. Int. J. Biol. Macromol. 208, 688–697. https://doi.org/10.1016/j.ijbiomac.2022.03.151.

Chmura, A., Rustler, S., Paravidino, M., van Rantwijk, F., Stolz, A., Sheldon, R.A., 2013. The combi-CLEA approach: enzymatic cascade synthesis of enantiomerically pure (*S*)-mandelic acid. Tetrahedron Asymmetry 24, 1225–1232. https://doi.org/10.1016/j.tetasy.2013.08.013.

Choi, J.-M., Han, S.-S., Kim, H.-S., 2015. Industrial applications of enzyme biocatalysis: current status and future aspects. Biotechnol. Adv. 33, 1443–1454. https://doi.org/10.1016/j.biotechadv.2015.02.014.

Di Cosimo, R., Mc Auliffe, J., Poulose, A.J., Bohlmann, G., 2013. Industrial use of immobilized enzymes. Chem. Soc. Rev. 42, 6437–6474. https://doi.org/10.1039/c3cs35506c.

Drufva, E.E., Spengler, N.R., Hix, E.G., Bailey, C.B., 2021. Site-directed mutagenesis of modular polyketide synthase ketoreductase domains for altered stereochemical control. Chembiochem 22, 1122–1150. https://doi.org/10.1002/cbic.202000613.

Fernández-Arrojo, L., Guazzaroni, M.-E., López-Cortés, N., Beloqui, A., Ferrer, M., 2010. Metagenomic era for biocatalyst identification. Curr. Opin. Biotechnol. 21, 725–733. https://doi.org/10.1016/j.copbio.2010.09.006.

Fernández-Lafuente, R., Rodriguez, V., Guisán, J.M., 1998. The coimmobilization of D-amino acid oxidase and catalase enables the quantitative transformation of D-amino acids (D-phenylalanine) into α-keto acids (phenylpyruvic acid). Enzyme Microb. Technol. 23, 28–33. https://doi.org/10.1016/S0141-0229(98)00028-3.

Fernandez-Lopez, L., Roda, S., Gonzalez-Alfonso, J.L., Plou, F.J., Guallar, V., Ferrer, M., 2022. Design and characterization of in-one protease-esterase pluriZyme. Int. J. Mol. Sci. 23. https://doi.org/10.3390/IJMS232113337.

France, S.P., Hepworth, L.J., Turner, N.J., Flitsch, S.L., 2017. Constructing biocatalytic cascades: In vitro and in vivo approaches to *de novo* multi-enzyme pathways. ACS Catal. 7, 710–724. https://doi.org/10.1021/acscatal.6b02979.

Høst, A.V., Morellon-Sterling, R., Carballares, D., Woodley, J.M., Fernandez-Lafuente, R., 2022. Co-enzymes with dissimilar stabilities: a discussion of the likely biocatalyst performance problems and some potential solutions. Catalysts 12, 1570. https://doi.org/10.3390/catal12121570.

Hwang, E.T., Lee, S., 2019. Multienzymatic cascade reactions via enzyme complex by immobilization. ACS Catal. 9, 4402–4425. https://doi.org/10.1021/acscatal.8b04921.

Idan, O., Hess, H., 2013a. Engineering enzymatic cascades on nanoscale scaffolds. Curr. Opin. Biotechnol. 24, 606–611. https://doi.org/10.1016/j.copbio.2013.01.003.
Idan, O., Hess, H., 2013b. Origins of activity enhancement in enzyme cascades on scaffolds. ACS Nano 7, 8658–8665. https://doi.org/10.1021/nn402823k.
Idan, O., Hess, H., 2012. Diffusive transport phenomena in artificial enzyme cascades on scaffolds. Nat. Nanotechnol. 7, 769–770. https://doi.org/10.1038/nnano.2012.222.
Liese, A., Hilterhaus, L., 2013. Evaluation of immobilized enzymes for industrial applications. Chem. Soc. Rev. 42, 6236–6249. https://doi.org/10.1039/c3cs35511j.
Lopez-Gallego, F., Schmidt-Dannert, C., 2010. Multi-enzymatic synthesis. Curr. Opin. Chem. Biol. 14, 174–183. https://doi.org/10.1016/j.cbpa.2009.11.023.
Mateo, C., Chmura, A., Rustler, S., Van Rantwijk, F., Stolz, A., Sheldon, R.A., 2006. Synthesis of enantiomerically pure *(S)*-mandelic acid using an oxynitrilase-nitrilase bienzymatic cascade: a nitrilase surprisingly shows nitrile hydratase activity. Tetrahedron Asymmetry 17, 320–323. https://doi.org/10.1016/j.tetasy.2006.01.020.
Monteiro, R.R.C., da Silva, S.S.O., Cavalcante, C.L., de Luna, F.M.T., Bolivar, J.M., Vieira, R.S., Fernandez-Lafuente, R., 2022. Biosynthesis of alkanes/alkenes from fatty acids or derivatives (triacylglycerols or fatty aldehydes). Biotechnol. Adv. 61, 108045. https://doi.org/10.1016/j.biotechadv.2022.108045.
Morellon-Sterling, R., Carballares, D., Arana-Peña, S., Siar, E.-H., Braham, S.A., Fernandez-Lafuente, R., 2021. Advantages of supports activated with divinyl sulfone in enzyme coimmobilization: Possibility of multipoint covalent immobilization of the most stable enzyme and immobilization via ion exchange of the least stable enzyme. ACS Sustain. Chem. Eng. 9, 7508–7518. https://doi.org/10.1021/acssuschemeng.1c01065.
Paschalidis, L., Arana-Peña, S., Sieber, V., Burger, J., 2023. Mechanistic modeling, parametric study, and optimization of immobilization of enzymatic cascades in porous particles. React. Chem. Eng. 8, 2234–2244. https://doi.org/10.1039/D3RE00072A.
Paschalidis, L., Beer, B., Sutiono, S., Sieber, V., Burger, J., 2022. Design of enzymatic cascade reactors through multi-objective dynamic optimization. Biochem. Eng. J. 181, 108384. https://doi.org/10.1016/j.bej.2022.108384.
Paschalidis, L., Fröschl, D., Ibañez, M., Sutiono, S., Sieber, V., Burger, J., 2024. Boosting of enzymatic cascades by intermediates: Theoretical analysis and model-based optimization. Biochem. Eng. J. 210, 109440. https://doi.org/10.1016/j.bej.2024.109440.
Pizarro, C., Brañes, M.C., Markovits, A., Fernández-Lorente, G., Guisán, J.M., Chamy, R., Wilson, L., 2012. Influence of different immobilization techniques for *Candida cylindracea* lipase on its stability and fish oil hydrolysis. J. Mol. Catal. B Enzym. 78, 111–118. https://doi.org/10.1016/j.molcatb.2012.03.012.
Ren, S., Li, C., Jiao, X., Jia, S., Jiang, Y., Bilal, M., Cui, J., 2019. Recent progress in multienzymes co-immobilization and multienzyme system applications. Chem. Eng. J. 373, 1254–1278. https://doi.org/10.1016/j.cej.2019.05.141.
Renata, H., Wang, Z.J., Arnold, F.H., 2015. Expanding the enzyme universe: Accessing non-natural reactions by mechanism-guided directed evolution. Angew. Chemie Int. Ed. 54, 3351–3367. https://doi.org/10.1002/anie.201409470.
Rodrigues, R.C., Barbosa, O., Ortiz, C., Berenguer-Murcia, Á., Torres, R., Fernandez-Lafuente, R., 2014. Amination of enzymes to improve biocatalyst performance: Coupling genetic modification and physicochemical tools. RSC Adv. 4, 38350–38374. https://doi.org/10.1039/c4ra04625k.
Rodrigues, R.C., Berenguer-Murcia, Á., Carballares, D., Morellon-Sterling, R., Fernandez-Lafuente, R., 2021. Stabilization of enzymes via immobilization: Multipoint covalent attachment and other stabilization strategies. Biotechnol. Adv. 52, 107821. https://doi.org/10.1016/j.biotechadv.2021.107821.
Rodrigues, R.C., Ortiz, C., Berenguer-Murcia, Á., Torres, R., Fernández-Lafuente, R., 2013. Modifying enzyme activity and selectivity by immobilization. Chem. Soc. Rev. 42, 6290–6307. https://doi.org/10.1039/c2cs35231a.
Schmid-Dannert, C., López-Gallego, F., 2019. Advances and opportunities for the design of self-sufficient and spatially organized cell-free biocatalytic systems. Curr. Opin. Chem. Biol. 49, 97–104. https://doi.org/10.1016/j.cbpa.2018.11.021.
Schrittwieser, J.H., Velikogne, S., Hall, M., Kroutil, W., 2018. Artificial biocatalytic linear cascades for preparation of organic molecules. Chem. Rev. 118, 270–348. https://doi.org/10.1021/acs.chemrev.7b00033.
Sheldon, R.A., Pereira, P.C., 2017. Biocatalysis engineering: the big picture. Chem. Soc. Rev. 46, 2678–2691. https://doi.org/10.1039/c6cs00854b.
Sheldon, R.A., van Pelt, S., 2013. Enzyme immobilisation in biocatalysis: why, what and how. Chem. Soc. Rev. 42, 6223–6235. https://doi.org/10.1039/C3CS60075K.
Sheldon, R.A., Woodley, J.M., 2018. Role of biocatalysis in sustainable chemistry. Chem. Rev. 118, 801–838. https://doi.org/10.1021/acs.chemrev.7b00203.
Upadhya, R., Nagajyothi, H., Bhat, S.G., 1999. *D*-Amino acid oxidase and catalase of detergent permeabilized *Rhodotorula gracilis* cells and its potential use for the synthesis of α-keto acids. Process Biochem. 35, 7–13. https://doi.org/10.1016/S0032-9592(99)00025-4.
Van Rantwijk, F., Mateo, C., Chmura, A., Fernandes, B.C.M., Sheldon, R.A., 2008. Nitrilases in the Enantioselective Synthesis of α-Hydroxycarboxylic Acids. Modern Biocatalysis. Wiley, pp. 261–272.
Velasco-Lozano, S., López-Gallego, F., 2018. Wiring step-wise reactions with immobilized multi-enzyme systems. Biocatal. Biotransform. 36, 184–194. https://doi.org/10.1080/10242422.2017.1310208.
Wahab, R.A., Elias, N., Abdullah, F., Ghoshal, S.K., 2020. On the taught new tricks of enzymes immobilization: an all-inclusive overview. React. Funct. Polym. 152, 104613. https://doi.org/10.1016/j.reactfunctpolym.2020.104613.
Woodley, J.M., 2022. Integrating protein engineering into biocatalytic process scale-up. Trends Chem. 4, 371–373. https://doi.org/10.1016/j.trechm.2022.02.007.
Wu, S., Snajdrova, R., Moore, J.C., Baldenius, K., Bornscheuer, U.T., 2021. Biocatalysis: enzymatic synthesis for industrial applications. Angew. Chemie Int. Ed. 60, 88–119. https://doi.org/10.1002/anie.202006648.
Xiong, Y., Tsitkov, S., Hess, H., Gang, O., Zhang, Y., 2022. Microscale colocalization of cascade enzymes yields activity enhancement. ACS Nano 16, 10383–10391. https://doi.org/10.1021/acsnano.2c00475.
Xu, K., Chen, X., Zheng, R., Zheng, Y., 2020. Immobilization of multi-enzymes on support materials for efficient biocatalysis. Front. Bioeng. Biotechnol. 8, 1–17. https://doi.org/10.3389/fbioe.2020.00660.
Zhang, Y., Tsitkov, S., Hess, H., 2016. Proximity does not contribute to activity enhancement in the glucose oxidase–horseradish peroxidase cascade. Nat. Commun. 7, 13982. https://doi.org/10.1038/ncomms13982.

Supporting figures.

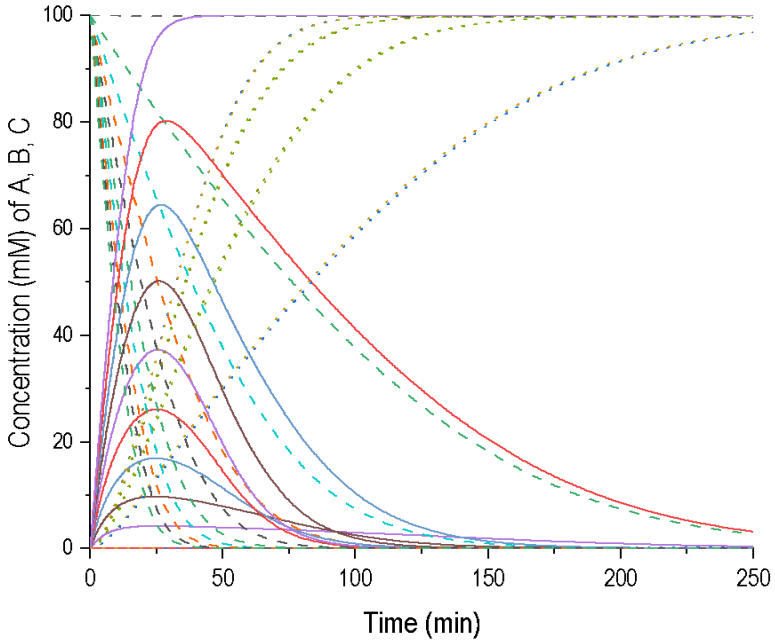

Figure S1: Effect of the enzyme ratio (E_1/E_T) in the reaction courses of the modification of A catalyzed by a mixture of free enzymes to minimize the reaction time required to reach 95% C yield, $K_{M1}=K_{M2}=50$. Dashed lines: Substrate A, solid lines: intermediate B and dotted lines: product C. Additional parameters: $Kcat_1= Kcat_2=10$, $E_T=1$.

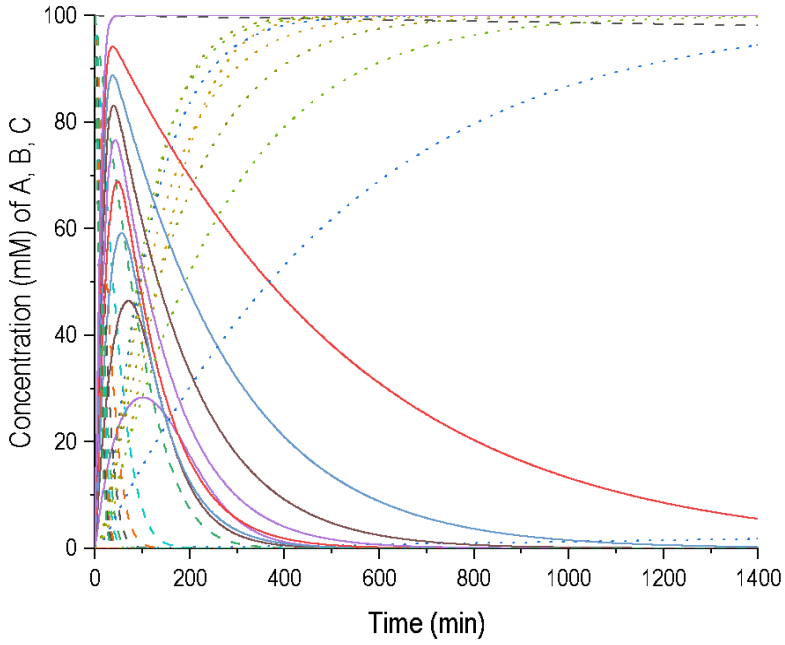

Figure S2: Effect of the enzyme ratio (E_1/E_T) in the reaction courses of the modification of A catalyzed by a mixture of free to minimize the reaction time required to reach 95% C yield, K_{M1}=50 and K_{M2}=500. Dashed lines: Substrate A, solid lines: intermediate B and dotted lines: product C. Additional parameters: $Kcat_1$= $Kcat_2$=10, E_T=1.

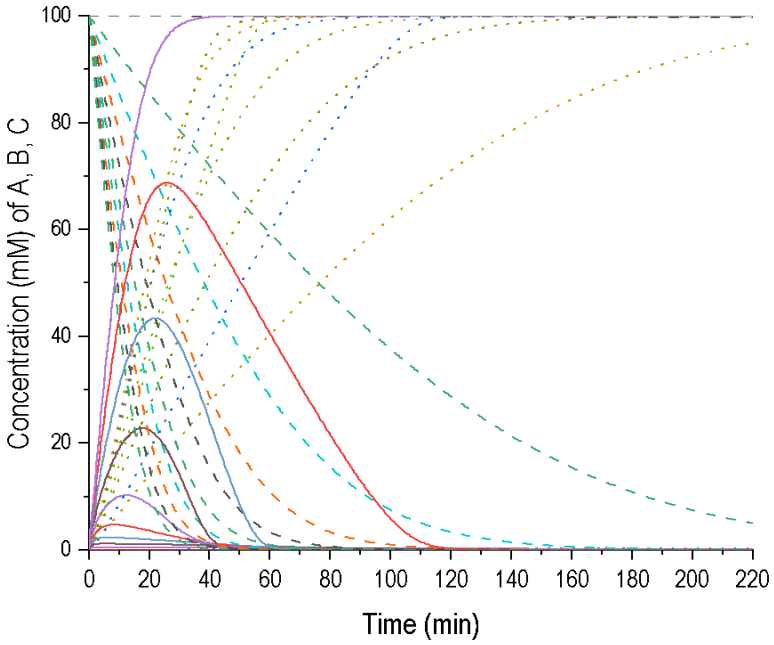

Figure S3: Effect of the enzyme ratio (E_1/E_T) in the reaction courses of the modification of A catalyzed by a mixture of free enzymes to minimize the reaction time required to reach 95% C yield, K_{M1}=50 and K_{M2}=5. Dashed lines: Substrate A, solid lines: intermediate B and dotted lines: product C. Additional parameters: $Kcat_1$= $Kcat_2$=10, E_T=1.

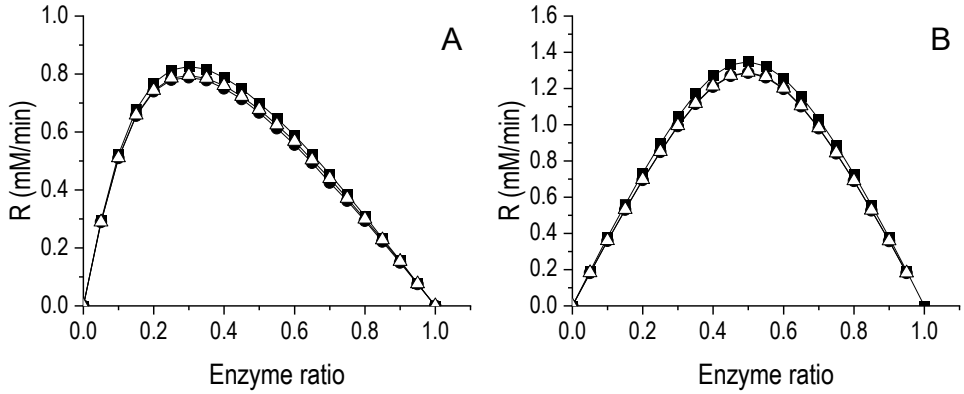

Figure S4: Effect of the enzymes ratio in the average rate of C formation using combi-biocatalysts without significant diffusional limitations and K_{M1}=K_{M2}=50: free enzymes mixtures (full line, full square), individually immobilized enzymes (full line, full circles) or co-immobilized enzymes (full line, empty triangles). **(A)**: At 20 % conversion of A and **(B)**: At 95 % yield of C. Additional parameters free enzymes mixtures: $Kcat_1$= $Kcat_2$=10, E_T=1, ϕ_{mod} = 2.7 10-3.

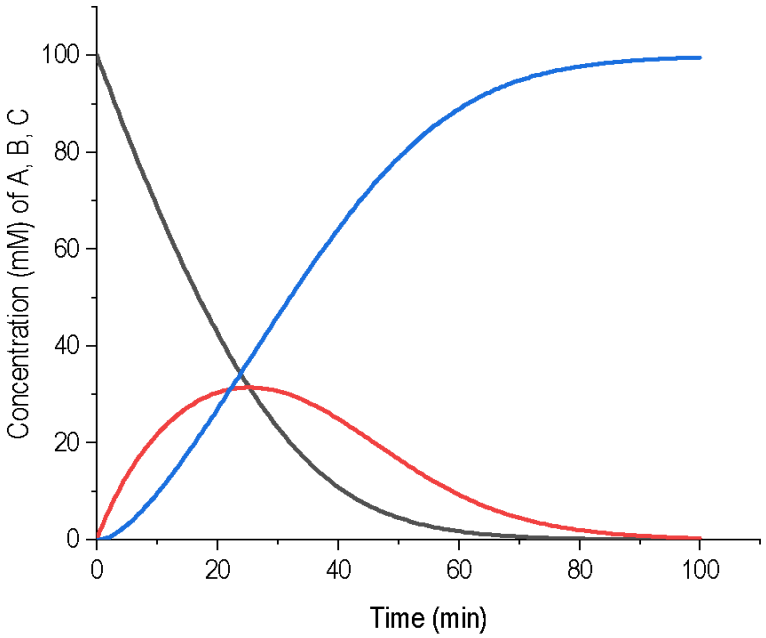

Figure S5: Reaction course of optimal combi-biocatalysts without significant diffusional limitations. Mixtures of free enzymes, individually immobilized enzymes and co-immobilized enzymes. Black lines: Substrate A; red lines: intermediate B and blue lines: product C. Additional parameters: $Kcat_1$=$Kcat_2$=10, E_T=1. Optimum V_{P1}/V_{Ptotal} =0.5. ϕ_{mod} = 2.7 10-3. Concentration time courses of A, B, C and overlap with intraparticle concentration under these conditions.

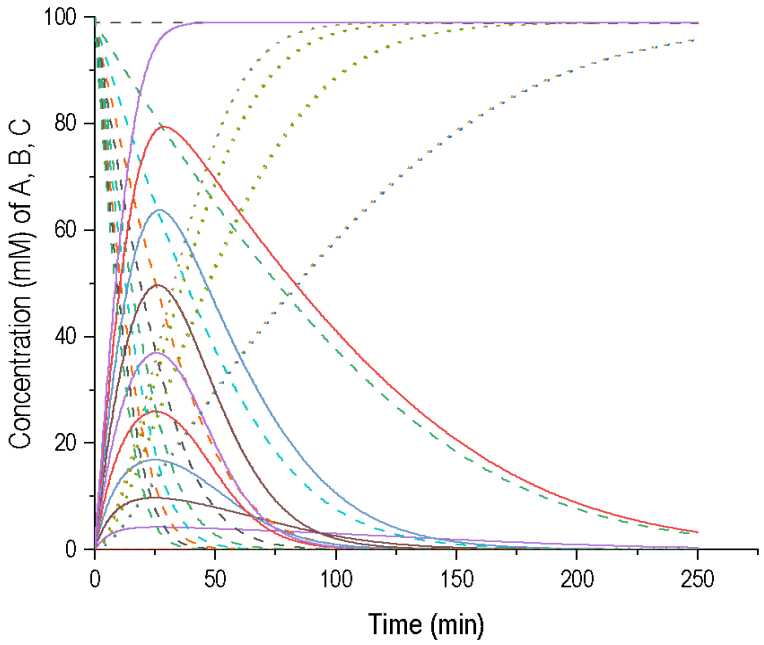

Figure S6: Effect of the enzyme ratio (V_{P1}/V_{Ptotal}) in the reaction courses of the modification of A catalyzed by an individually immobilized enzyme to minimize the reaction time required to reach 95% C yield, $K_{M1}=K_{M2}=50$ without diffusional limitations. Dashed lines: Substrate A, solid lines: intermediate B and dotted lines: product C. Additional parameters: $Kcat_1= Kcat_2=10$, $E_T=1$, ϕ_{mod} = 2.7 10^{-3}.

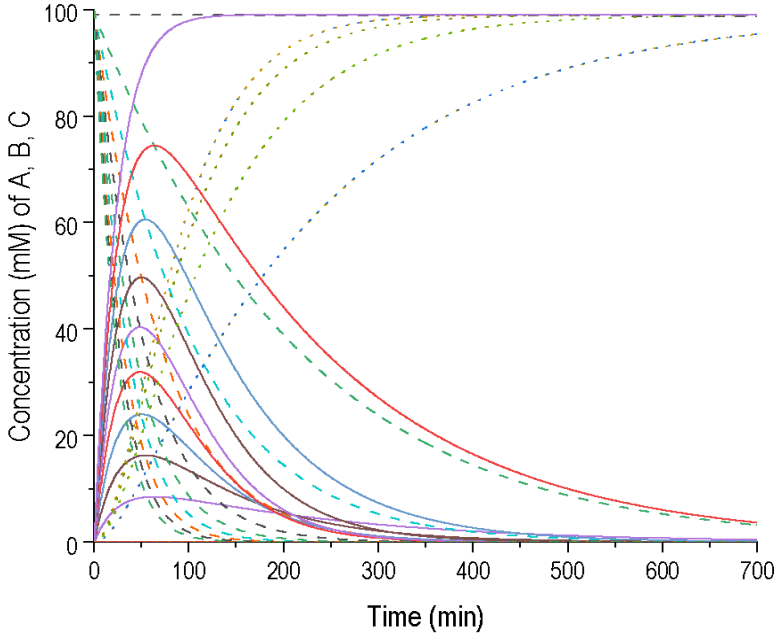

Figure S7: Effect of the enzyme ratio (V_{P1}/V_{Ptotal}) in the reaction courses of the modification of A catalyzed by an individually immobilized enzyme to minimize the reaction time required to reach 95% C yield, $K_{M1}=K_{M2}=50$ with diffusional limitations. Dashed lines: Substrate A, solid lines: intermediate B and dotted lines: product C. Additional parameters: $Kcat_1=Kcat_2=10$, $E_1=E_2=100$, $\phi_{mod} = 1.1$.

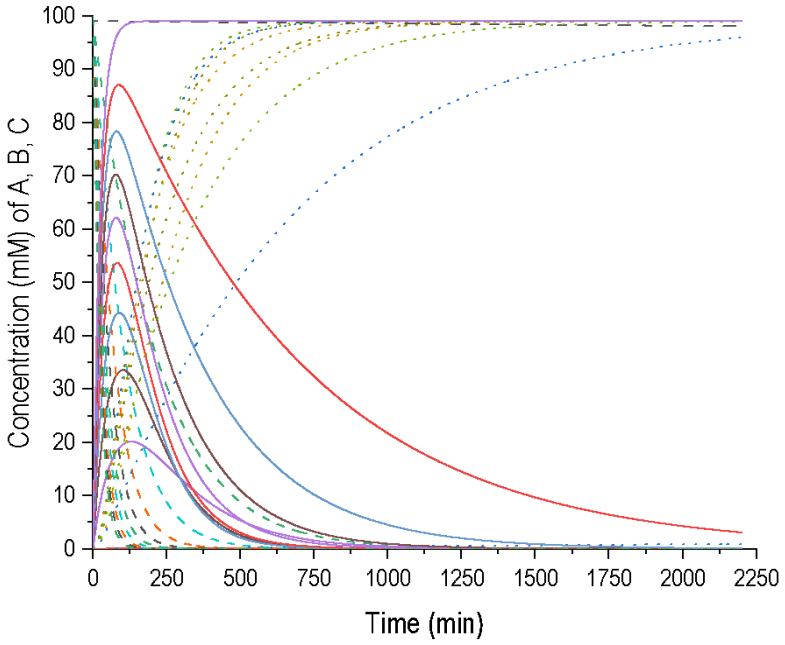

Figure S8: Effect of the enzyme ratio (V_{P1}/V_{Ptotal}) in the reaction courses of the modification of A catalyzed by an individually immobilized enzyme to minimize the reaction time required to reach 95% C yield, K_{M1}=50 and K_{M2}=500 with diffusional limitations. Dashed lines: Substrate A, solid lines: intermediate B and dotted lines: product C. Additional parameters: $Kcat_1$=$Kcat_2$=10, E_1=E_2=100, ϕ_{mod} = 1.1.

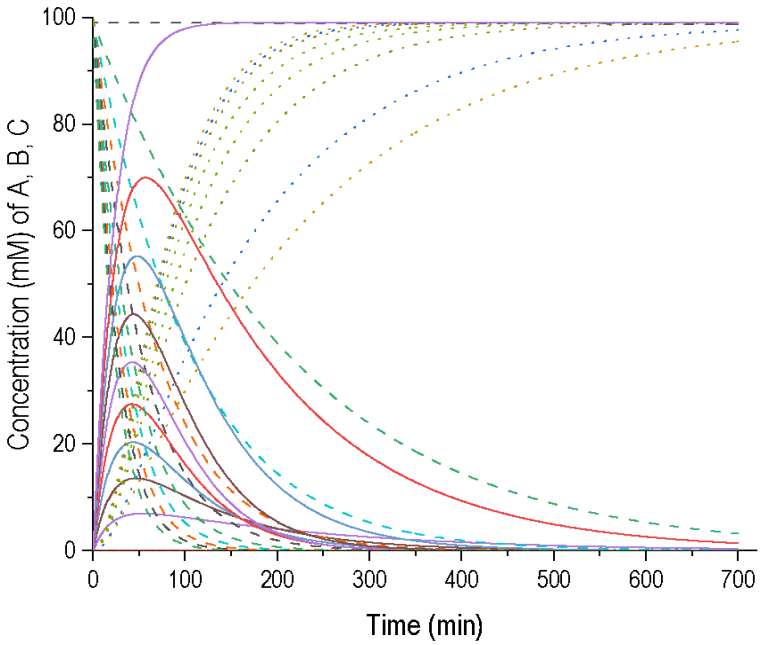

Figure S9: Effect of the enzyme ratio (V_{P1}/V_{Ptotal}) in the reaction courses of the modification of A catalyzed by an individually immobilized enzyme to minimize the reaction time required to reach 95% C yield, K_{M1}=50 and K_{M2}=5 with diffusional limitations. Dashed lines: Substrate A, solid lines: intermediate B and dotted lines: product C. Additional parameters: $Kcat_1$=$Kcat_2$=10, E_1=E_2=100, ϕ_{mod} = 1.1.

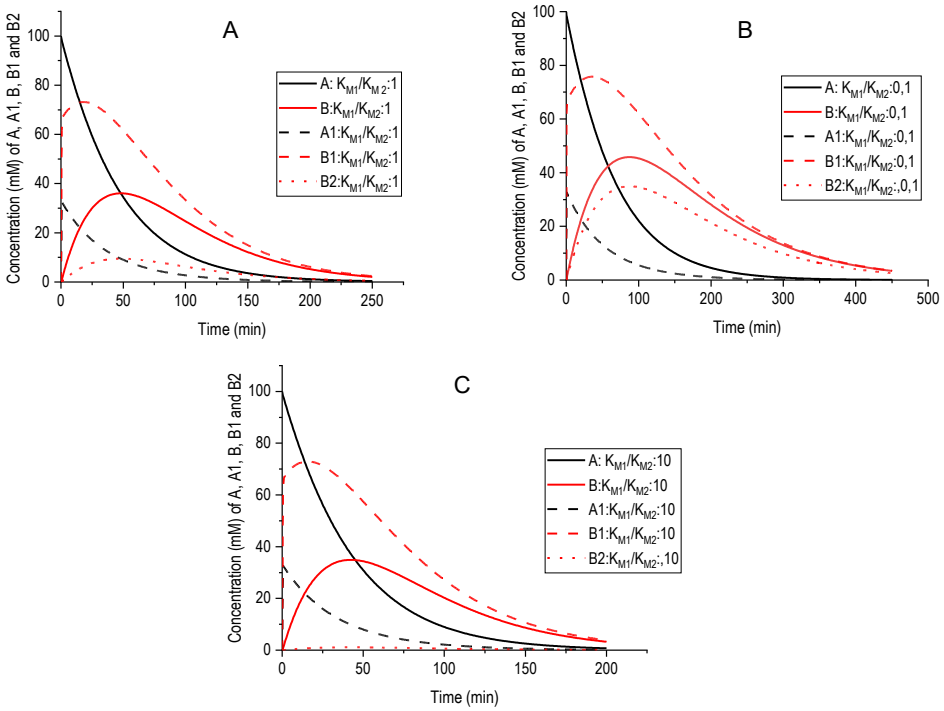

Figure S10: Effect of the enzymes K_{M1} and K_{M2} in the reaction courses of the modification of A catalyzed by the respective optimal combi-biocatalysts prepared using individually immobilized enzymes with diffusion matters to minimize the reaction time required to reach 95% C yield under the condition of A_0/K_M=2: K_{M1}= K_{M2}=50 (A); K_{M1}=50 and K_{M2}=500 (B), K_{M1}=50 and K_{M2}=5 (C). Black and solid lines: Substrate A; black and dashed lines: Substrate A1; red and solid lines: intermediate B; red and dashed lines: intermediate B1 and red and dotted lines: intermediate B2. Additional parameters: $Kcat_1$=$Kcat_2$=10, E_T=1. ϕ_{mod} = 1.1. Optimum V_{P1}/V_{Ptotal} (K_{M1}= K_{M2}=50) =0.5; K_{M1}=50 and K_{M2}=500) =0.35; (K_{M1}=50 and K_{M2}=5) = 0.55.

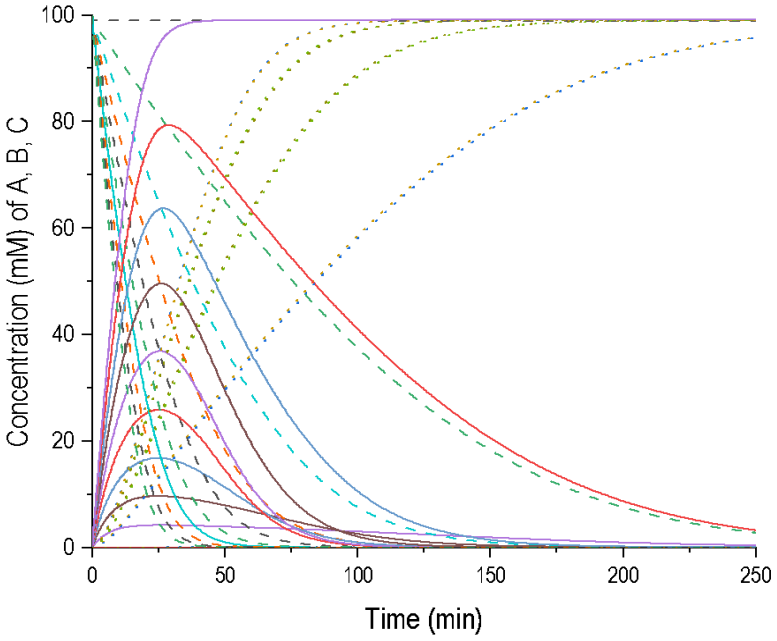

Figure S11: Effect of the enzyme ratio (V_{P1}/V_{Ptotal}) in the reaction courses of the modification of A catalyzed by a co-immobilized enzyme to minimize the reaction time required to reach 95% C yield, $K_{M1}=K_{M2}=50$ without diffusional limitations. Dashed lines: Substrate A, solid lines: intermediate B and dotted lines: product C. Additional parameters free enzymes mixtures: $Kcat_1=Kcat_2=10$, $E_T=1$, $\phi_{mod} = 2.7\ 10^{-3}$.

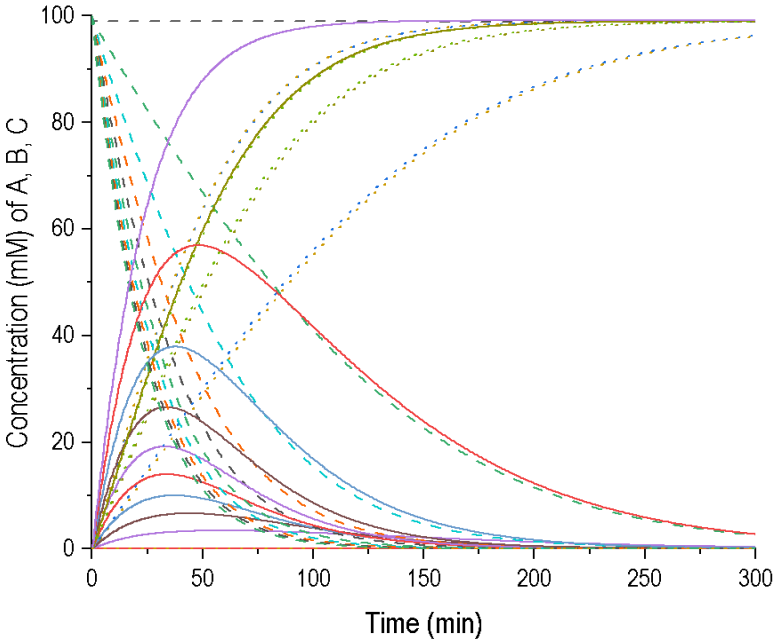

Figure S12: Effect of the enzyme ratio (V_{P1}/V_{Ptotal}) in the reaction courses of the modification of A catalyzed by a co-immobilized enzyme to minimize the reaction time required to reach 95% C yield, $K_{M1}=K_{M2}=50$ with diffusional limitations. Dashed lines: Substrate A, solid lines: intermediate B and dotted lines: product C. Additional parameters: $Kcat_1=Kcat_2=10$, $E_T=100$, $\phi_{mod}= 1.1$.

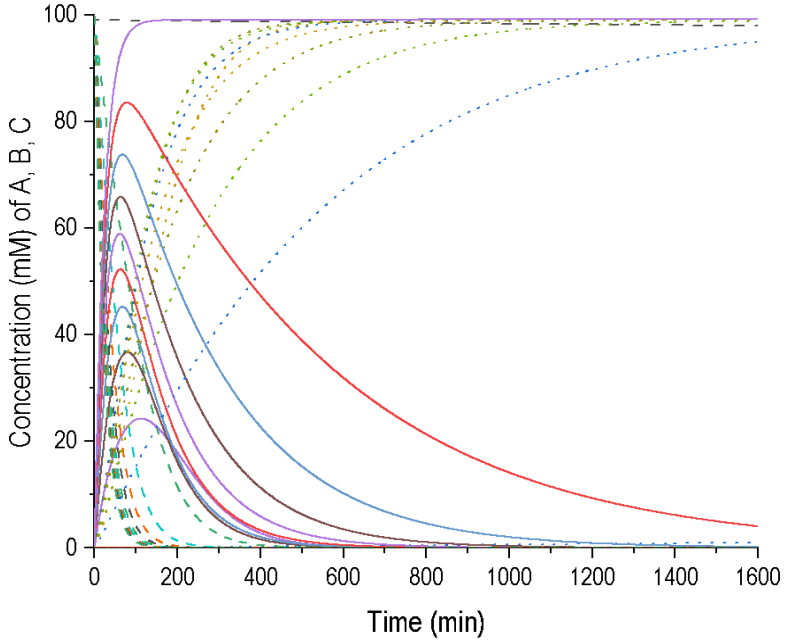

Figure S13: Effect of the enzyme ratio (V_{P1}/V_{Ptotal}) in the reaction courses of the modification of A catalyzed by a co-immobilized enzyme to minimize the reaction time required to reach 95% C yield, K_{M1}=50 and K_{M2}=500 with diffusional limitations. Dashed lines: Substrate A, solid lines: intermediate B and dotted lines: product C. Additional parameters: $Kcat_1$=$Kcat_2$=10, E_T=100, ϕ_{mod}= 1.1.

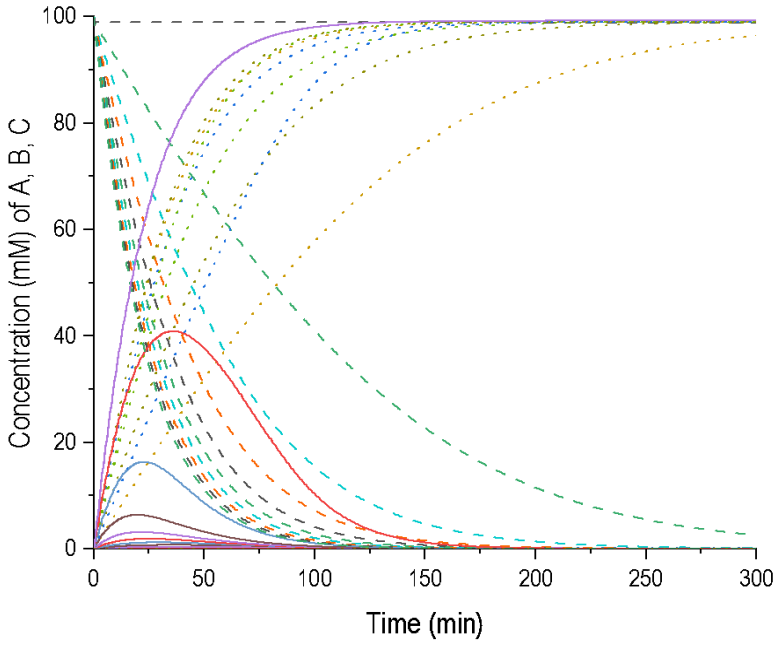

Figure S14: Effect of the enzyme ratio (V_{P1}/V_{Ptotal}) in the reaction courses of the modification of A catalyzed by a co-immobilized enzyme to minimize the reaction time required to reach 95% C yield, K_{M1}=50 and K_{M2}=5 with diffusional limitations. Dashed lines: Substrate A, solid lines: intermediate B and dotted lines: product C. Additional parameters: $Kcat_1$=$Kcat_2$=10, E_T=100, ϕ_{mod}= 1.1.

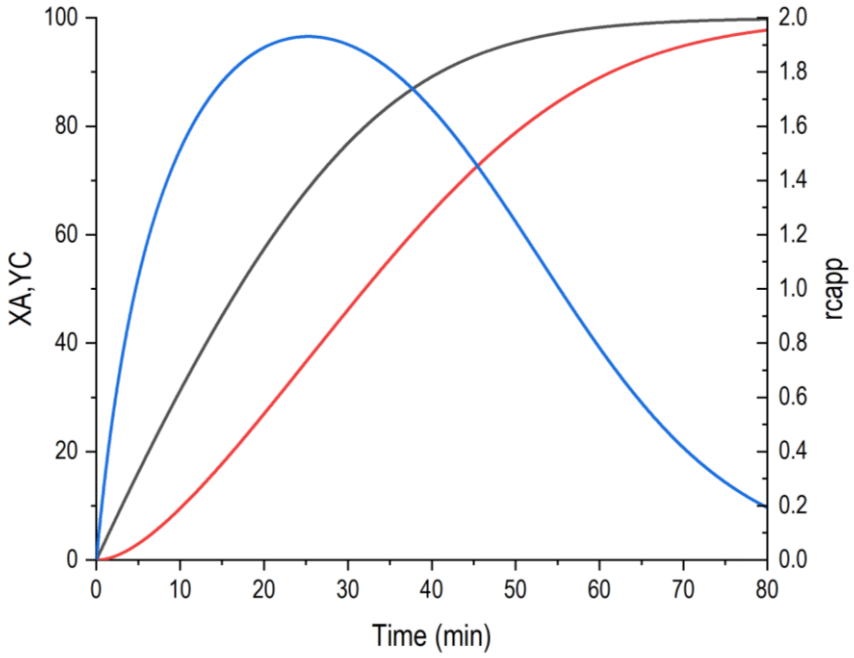

Figure S15: Effect of the enzymes K_{M1} and K_{M2} in the values of XA, YC and rcapp by the respective optimal combi-biocatalysts prepared using mixtures of free enzymes, individually immobilized enzymes and co-immobilized enzymes (K_{M1}=K_{M2}=50) without diffusional limitations. Red line: YC; blue line: rcapp and black line: XA.

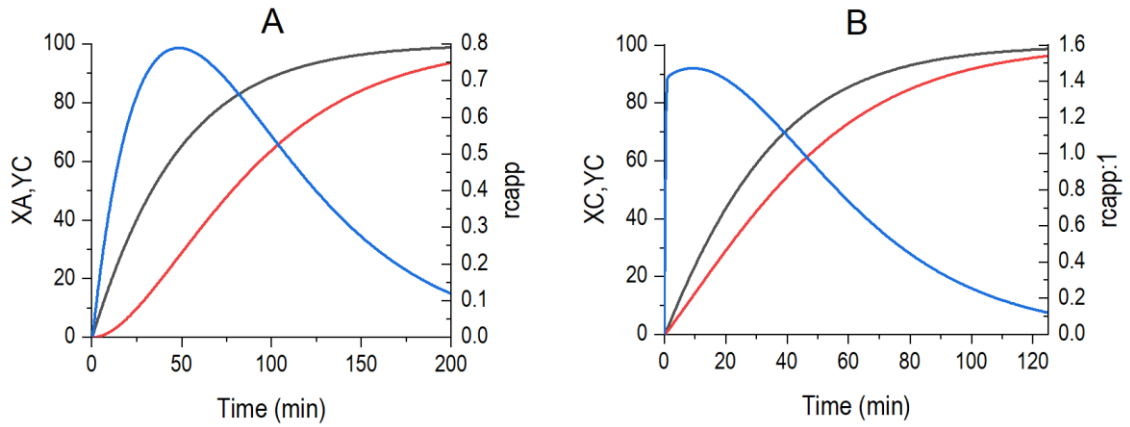

Figure S16: Effect of the enzymes K_{M1} and K_{M2} in the values of XA, YC and rcapp by the respective optimal combi-biocatalysts prepared using individually immobilized enzymes **(A)** and co-immobilized enzymes **(B)** (K_{M1}=K_{M2}=50) with diffusional limitations. Red line: YC; blue line: rcapp and black line: XA.

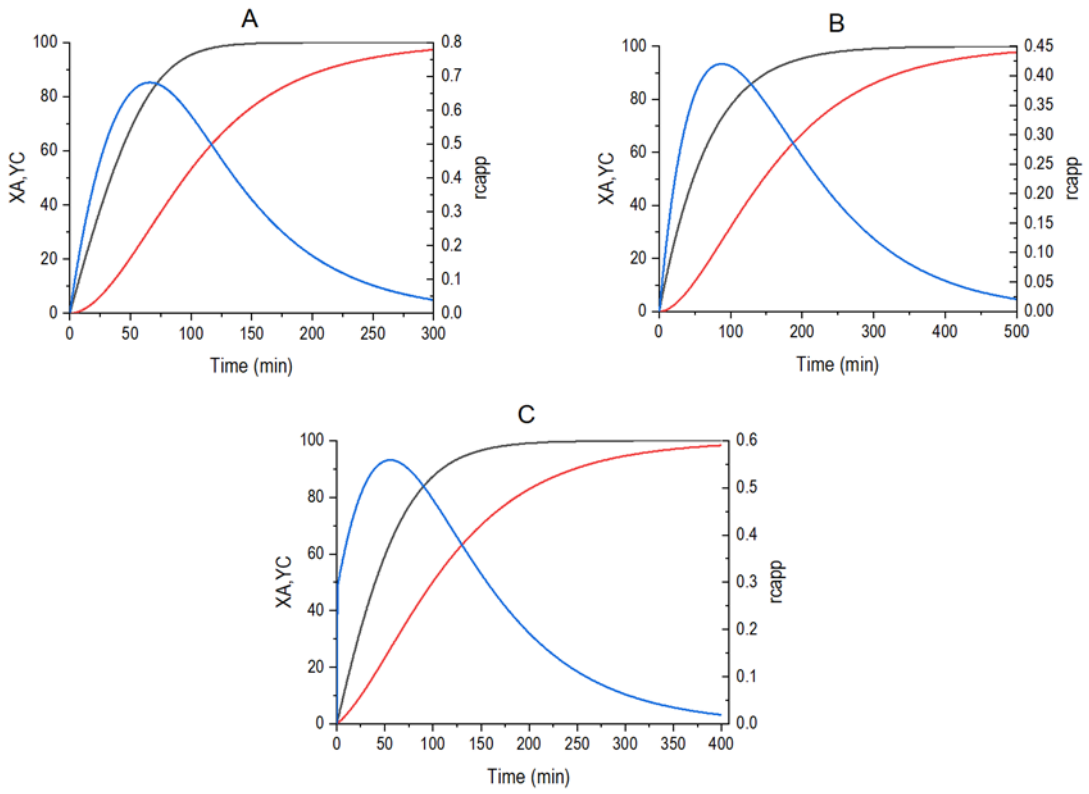

Figure S17: Effect of the enzymes K_{M1} and K_{M2} in the values of XA, YC and rcapp by the respective optimal combi-biocatalysts prepared using mixtures of free enzymes **(A)**, individually immobilized enzymes **(B)** and co-immobilized enzymes **(C)** (K_{M1}=50 and K_{M2}=500) with diffusional limitations. Red line: YC; blue line: rcapp and black line: XA.

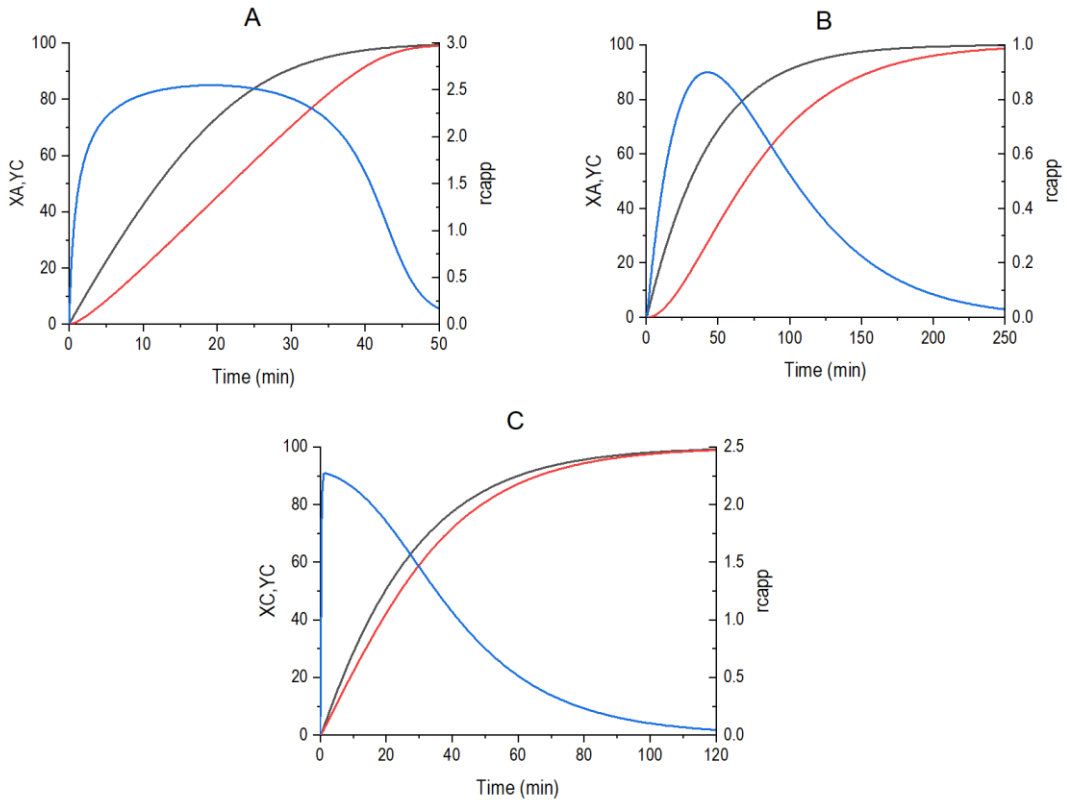

Figure S18: Effect of the enzymes K_{M1} and K_{M2} in the values of XA, YC and rcapp by the respective optimal combi-biocatalysts prepared using mixtures of free enzymes **(A)**, individually immobilized enzymes **(B)** and co-immobilized enzymes **(C)** (K_{M1}=50 and K_{M2}=5) with diffusional limitations. Red line: YC; blue line: rcapp and black line: XA.

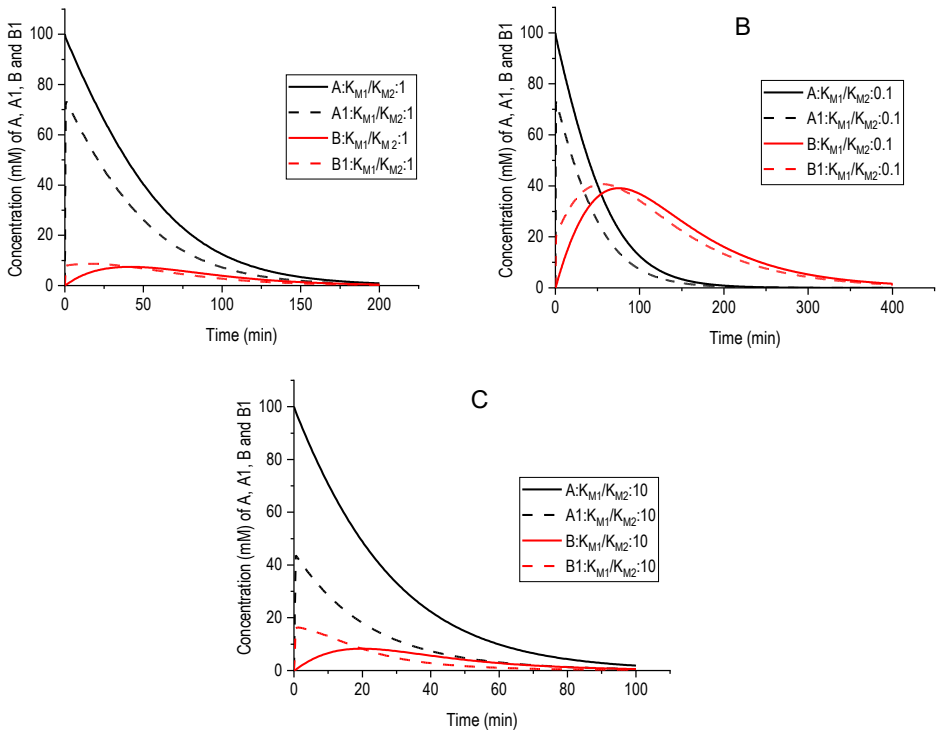

Figure S19: Effect of the enzymes K_{M1} and K_{M2} in the reaction courses of the modification of A catalyzed by the respective optimal combi-biocatalysts prepared using co-immobilized enzymes with diffusion matters to minimize the reaction time required to reach 95% C yield under the condition of A_0/K_M=2: K_{M1}= K_{M2}=50 (A); K_{M1}=50 and K_{M2}=500 (B), K_{M1}=50 and K_{M2}=5 (C). Black and solid lines: Substrate A; black and dashed lines: Substrate A1; red and solid lines: intermediate B and red and dashed lines: intermediate B1. Additional parameters: $Kcat_1$=$Kcat_2$=10, E_T=1. ϕ_{mod} = 1.1. Optimum V_{P1}/V_{Ptotal} (K_{M1}= K_{M2}=50) =0.5; K_{M1}=50 and K_{M2}=500) =0.25; (K_{M1}=50 and K_{M2}=5) = 0.6.

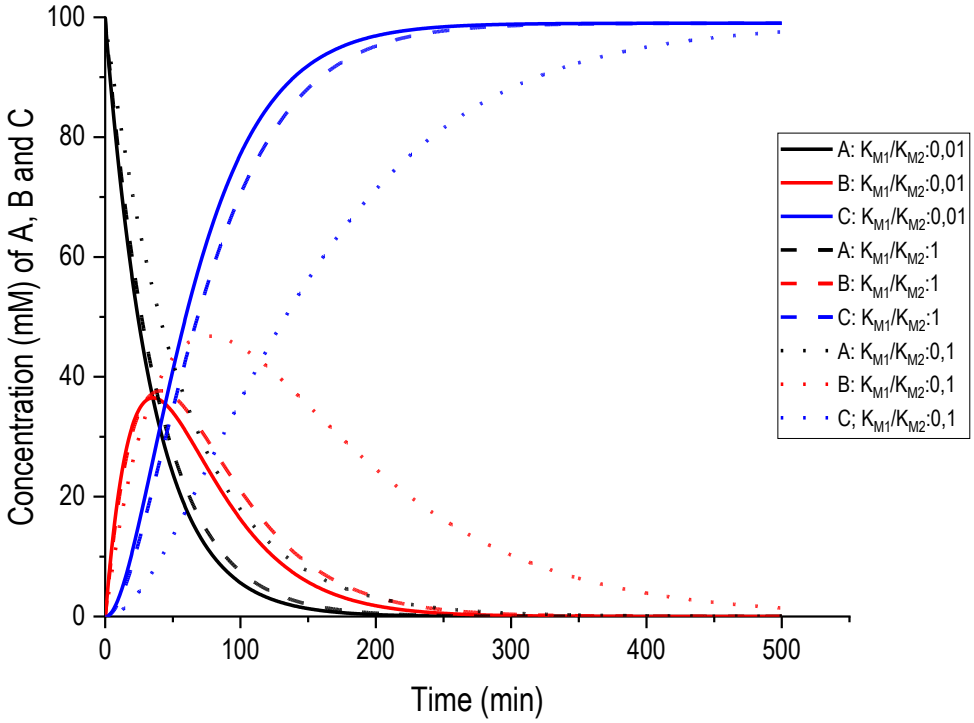

Figure S20: Effect of the enzymes K_{M1} and K_{M2} in the reaction courses of the modification of A catalyzed by the respective optimal combi-biocatalysts prepared using individually immobilized enzymes with diffusional limitations to minimize the reaction time required to reach 95% C yield under the condition of A_0/K_M=20: K_{M1}=5 and K_{M2}=500 (solid line); K_{M1}=5 and K_{M2}=5 (dashed lines), K_{M1}=5 and K_{M2}=50 (dotted lines). Black lines: Substrate A; red lines: intermediate B and blue lines: product C.

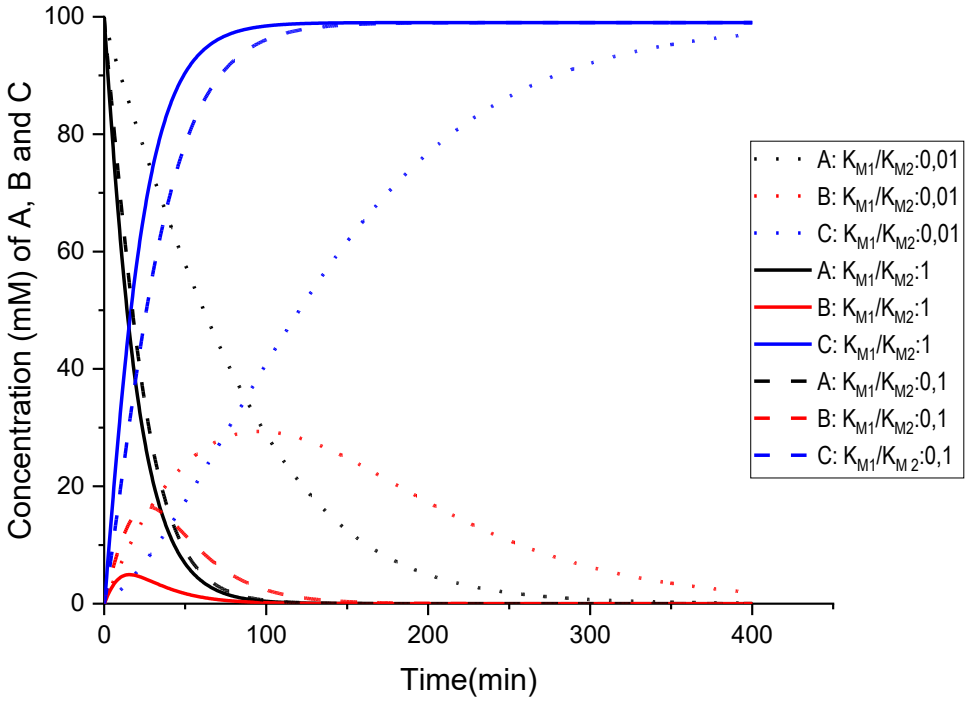

Figure S21: Effect of the enzymes K_{M1} and K_{M2} in the reaction courses of the modification of A catalyzed by the respective optimal combi-biocatalysts prepared using co-immobilized enzymes with diffusional limitations to minimize the reaction time required to reach 95% C yield under the condition of A_0/K_M=20: K_{M1}=5 and K_{M2}=500 (solid line); K_{M1}=5 and K_{M2}=5 (dashed lines), K_{M1}=5 and K_{M2}=50 (dotted lines). Black lines: Substrate A; red lines: intermediate B and blue lines: product C.